


## Notch and Aryl Hydrocarbon Receptor Signaling Impact Definitive Hematopoiesis from Human Pluripotent Stem Cells

AMY LEUNG,<sup>a,b</sup> ELIZABETH ZULICK,<sup>a,b</sup> NICHOLAS SKVIR,<sup>a,b</sup> KIM VANUYTSEL,<sup>a,b</sup> TASHA A. MORRISON,<sup>a</sup> ZAW HTUT NAING,<sup>a,b</sup> ZHONGYAN WANG,<sup>c</sup> YAN DAI,<sup>a</sup> DAVID H. K. CHUI,<sup>a</sup> MARTIN H. STEINBERG,<sup>a</sup> DAVID H. SHERR,<sup>c</sup> GEORGE J. MURPHY <sup>a,b</sup>

**Key Words.** Pluripotent stem cells • Definitive hematopoiesis • Notch signaling • Aryl hydrocarbon receptor signaling • Hematopoietic stem-progenitor cells • Regenerative medicine

<sup>a</sup>Section of Hematology and Oncology, Department of Medicine, Boston University School of Medicine, Boston, Massachusetts, USA; <sup>b</sup>Center for Regenerative Medicine (CRoM), Boston University and Boston Medical Center, Boston, Massachusetts, USA; <sup>c</sup>Department of Environmental Health, Boston University School of Public Health, Boston, Massachusetts, USA

Correspondence: George J. Murphy, Ph.D., Center for Regenerative Medicine, Boston University School of Medicine, 670 Albany Street, Suite 208, Boston, Massachusetts, 02118, USA. Telephone: 617-638-7541; e-mail: gjmurphy@bu.edu

Received September 19, 2017; accepted for publication March 13, 2018; first published online in *STEM CELLS EXPRESS* March 23, 2018.

<http://dx.doi.org/10.1002/stem.2822>

This is an open access article under the terms of the Creative Commons Attribution-NonCommercial License, which permits use, distribution and reproduction in any medium, provided the original work is properly cited and is not used for commercial purposes.

This article was published online on 1 April 2018. An error was subsequently identified. This notice is included in the online and print versions to indicate that both have been corrected 11 April 2018.

### ABSTRACT

Induced pluripotent stem cells (iPSCs) stand to revolutionize the way we study human development, model disease, and eventually, treat patients. However, these cell sources produce progeny that retain embryonic and/or fetal characteristics. The failure to mature to definitive, adult-type cells is a major barrier for iPSC-based disease modeling and drug discovery. To directly address these concerns, we have developed a chemically defined, serum and feeder-free-directed differentiation platform to generate hematopoietic stem-progenitor cells (HSPCs) and resultant adult-type progeny from iPSCs. This system allows for strict control of signaling pathways over time through growth factor and/or small molecule modulation. Through direct comparison with our previously described protocol for the production of primitive wave hematopoietic cells, we demonstrate that induced HSPCs are enhanced for erythroid and myeloid colony forming potential, and strikingly, resultant erythroid-lineage cells display enhanced expression of adult  $\beta$  globin indicating definitive pathway patterning. Using this system, we demonstrate the stage-specific roles of two key signaling pathways, Notch and the aryl hydrocarbon receptor (AHR), in the derivation of definitive hematopoietic cells. We illustrate the stage-specific necessity of Notch signaling in the emergence of hematopoietic progenitors and downstream definitive, adult-type erythroblasts. We also show that genetic or small molecule inhibition of the AHR results in the increased production of CD34<sup>+</sup>CD45<sup>+</sup> HSPCs while conversely, activation of the same receptor results in a block of hematopoietic cell emergence. Results presented here should have broad implications for hematopoietic stem cell transplantation and future clinical translation of iPSC-derived blood cells. *STEM CELLS* 2018;36:1004–1019

### SIGNIFICANCE STATEMENT

Induced pluripotent stem cells (iPSCs) stand to revolutionize the way we study human development, model disease, and eventually, treat patients. However, these cell sources produce progeny that retain primitive characteristics, a major barrier for disease modeling and drug discovery. We have developed a differentiation platform to create hematopoietic stem-progenitor cells from iPSCs that can produce adult-type blood cells. We demonstrate the stage-specific roles of two key signaling pathways, Notch and the aryl hydrocarbon receptor, in the derivation of definitive hematopoietic cells. These results have broad implications for hematopoietic stem cell transplantation and clinical translation of iPSC-derived blood cells.

### INTRODUCTION

A long-standing goal of developmental hematologists has been the derivation of non-genetically modified hematopoietic stem-progenitor cells (HSPCs) from embryonic stem cell (ESC) or induced pluripotent stem cell (iPSC) sources. These HSPCs should be capable of generating all adult hematopoietic cell lineages and

contribute to long-term repopulating hematopoiesis in vivo. Despite extensive efforts, this goal has not yet been achieved, likely due to an incomplete understanding of the complex regulatory processes involved in the specification and maintenance of these cells during embryogenesis, and later, in the adult bone marrow (BM). Complicating the issue, there are known differences in the differentiation and

engraftment capabilities of fetal and adult-stage HSPCs [1, 2] and these developmentally distinct HSPCs likely require unique maintenance and specification conditions. Moreover, HSPC heterogeneity has been observed with purified, tissue-specific HSPCs, suggesting that there are complex intrinsic or extrinsic factors that may influence HSPC functionality [3–6].

To date, primitive erythroid, myeloid, and lymphoid-lineage hematopoietic cells have been successfully generated from human PSCs (hPSCs) using a variety of embryoid body (EB), monolayer, serum-dependent, and serum-free differentiation methods [7–12]. This suggests that it is technically possible to generate cells analogous to yolk sac primitive, yolk sac definitive, and also possibly intra-embryonic definitive hematopoietic cells from hPSCs. However, notably, the hematopoietic progenitors generated from both murine and human ESCs and iPSCs demonstrate extremely limited engraftment potential compared with native HSPCs, an indication that cells fulfilling the most stringent criteria for HSPC functionality have yet to be generated from PSC sources. This point is highlighted by the fact that hPSC-derived hematopoietic cells possess predominantly primitive/early developmental characteristics with hPSC-derived erythroid cells (Erys) exhibiting mainly embryonic and early fetal characteristics with an inability to progress toward adult-stage cells. Multiple protocols for the production of PSC-derived erythroid-lineage cells have been characterized, and all describe the formation of hemoglobinized but developmentally blocked erythrocytes that are mostly nucleated and predominantly express embryonic (HbE:  $\zeta$ ,  $\epsilon$ ) and fetal (HbF,  $\gamma$ ) globins. These cells are developmentally analogous to erythrocytes found in embryonic circulation, the embryonic yolk sac and in the developing fetal liver (FL) [10, 11, 13]. In contrast, adult Erys generated from post-natal BM erythroid progenitor cells express adult (HbA) hemoglobin (Hb) comprised of alpha (HBA,  $\alpha$ ) and beta (HBB,  $\beta$ ) chains, enucleate more efficiently, and adopt a classic biconcave shape in circulation [14]. The current inability to produce hPSC-derived definitive, end-stage erythrocytes is a roadblock for many promising applications of hPSC technologies in the study of erythropoiesis, such as the disease modeling of  $\beta$ -hemoglobinopathies (sickle cell disease [SCD] and  $\beta$ -thalassemia) with patient-derived iPSCs. Notably, two recent high-profile publications have demonstrated the production of HSPCs with long-term engraftment potential and the ability to produce “adult-type” cells via the overexpression of multiple transcription factors in PSC-derived putative hemogenic endothelium [15, 16]. Transcription factor-mediated reprogramming confers hPSC-derived Erys with some measure of globin-switching ability, with cells expressing levels of  $\beta$ -globin similar to cord blood erythrocytes [16, 17]. Although these approaches are promising for near-term clinical application, they further demonstrate the inability to recapitulate the natural developmental cascade required to produce such cells from PSCs. Ideally, an optimal differentiation system would induce the natural, progressive molecular and transcriptional changes that occur during the switch from primitive to definitive hematopoiesis, without the need for extraneous genetic manipulations.

The signaling events that drive the commitment of pluripotent cells to early hematopoietic tissues are well-defined [18–20] and can be replicated in a controlled manner with serum-free, cytokine-dependent differentiation conditions. The

importance of mesodermal patterning for the efficient derivation of hematopoietic cell types of interest has been highlighted by studies of ActivinA/Nodal/TGF $\beta$  and Wnt signaling in the differential specification of hematopoietic mesoderm toward primitive versus definitive hematopoietic cell fates [7, 8, 21].

The first HSCs during embryogenesis arise in the aorta–gonad–mesonephros (AGM region) from the endothelial cells lining the ventral wall of the dorsal aorta through the process of endothelial-to-hematopoietic transition (EHT) [22–24]. Notch is a key signaling pathway in this process and its ablation prevents definitive AGM hematopoiesis in vertebrates but is dispensable for primitive/yolk sac-stage hematopoiesis [25–29]. A comparison of definitive murine HSPCs in vivo with murine ESC (mESC)-derived hematopoietic progenitors in vitro showed under-representation of Notch pathway gene expression in ESC-derived cells [30]. Notably, primate PSCs differentiated in contact with Notch-ligand expressing endothelial cells demonstrated enhanced engraftment potential in recipient mice [31] highlighting the potential impact of this pathway on the ability to generate de novo HSPCs in vitro.

While we have characterized the ability of aryl hydrocarbon receptor (AHR) signaling activation to drive hPSC-*primitive* hematopoietic progenitor cell expansion [32], this signaling pathway also plays a key role in normal HSPC physiology. In the murine knockout (KO) model, young AHR<sup>-/-</sup> mice have a circadian-rhythm associated twofold increase in LT-HSC and white blood cell compartments (myeloid and lymphoid cells) [33, 34], while aged AHR<sup>-/-</sup> mice display a HSC exhaustion and myeloproliferative disorder phenotype [35]. Interestingly, a small-molecule AHR inhibitor, SR-1, was able to expand CD34<sup>+</sup> primary cord blood HSPCs ex vivo [36], and UM171, which also acts as an AHR modulator, has a similar effect both alone and together with SR-1 [37, 38]. Recent studies also suggest that AHR inhibition increases hematoendothelial/HSPC generation from human PSCs [39, 40]. The mechanisms through which AHR controls these different hematopoietic processes are not well-defined. These studies highlight the potential multifaceted, differential roles for the AHR spanning both primitive and definitive hematopoiesis.

In this study, we harness a chemically defined, serum and feeder-free hPSC hematopoietic differentiation system to interrogate the molecular mechanisms and signaling pathways controlling hematopoietic progenitor cell generation. We use this system to efficiently generate human hematopoietic cells from human iPSCs (hiPSCs) with characteristics of HSPCs. These cells exhibit enhanced erythroid and myeloid colony forming potential, and are able to generate progeny with definitive, adult-type characteristics including the expression of adult globin, suggesting patterning toward the definitive hematopoietic pathway. We highlight the critical importance of Notch signaling in the emergence of putative HSPCs and resultant adult-type erythroblasts from iPSCs. Moreover, using genetic and small molecule approaches to modulate AHR signaling, we illustrate the stage-specific effect of the receptor on the expansion and maintenance of HSPCs. We directly compare iPSC-derived primitive versus putative definitive hematopoietic progenitor cells from the same parental lines to examine the differential signaling, expression patterning, and functionality of these two populations. The presented studies have implications for the ex vivo manipulation of HSCs

from primary human sources and de novo generation of hPSC-derived HSPCs.

## MATERIALS AND METHODS

### iPSC Generation and Maintenance

hiPSCs (BU5, BU6, and BS31) were generated by hSTEMCCA lentiviral transduction of human peripheral blood mononuclear cells as described previously [41, 42]. iPSCs were maintained in mTESR (StemCell Technologies, Vancouver, Canada) on matrigel optimized for hPSC growth (Corning, Corning, NY Matrigel hESC-qualified Matrix, #354277) and passaged approximately every 7–8 days through ReLeSR (StemCell Tech., Vancouver, Canada) dissociation, following manufacturer instructions.

### CRISPR-Cas9 Generation of AHR KO Lines

AHR KO lines were created using lentiCRISPR v2 (Addgene no. 52961, Cambridge, MA), which contains Cas9 and a guide RNA cloning site (BsmBI). The two target sequences (5'-CCT-ACGCCAGTCGCAAGCGG-3' and 5'-CCGAGCGCGTCTCATCGCG-3', NM\_001621), selected by CRISPR designer (<http://crispr.mit.edu>), are located in the first exon of the *AHR*. The construction was confirmed by DNA sequence analysis using a WPRE-R primer (5'-CATAGCGTAAAGGAGCAACA). Cells were selected for 10 days with 1.0  $\mu\text{g/ml}$  puromycin. AHR KO was confirmed by Western blotting: AHR (1:1,000, 13,790; Cell Signaling Technologies, Danvers, MA) and  $\beta$ -actin-specific antibody (1:2,000, A5441; Sigma-Aldrich, St. Louis, MO) for loading control.

### Generation of Hematopoietic Cells from iPSC

iPS-megakaryocyte-erythroid progenitor (MEP) cells were generated as described previously [32]. D15/D16 suspension MEP hematopoietic cells were cultured for an additional 5 days in erythroid maturation media [IMDM (Thermo Fisher, Waltham, MA), 5% protein-free hybridoma media (PFHM-II, Thermo Fisher, Waltham, MA), 50  $\mu\text{g/ml}$  ascorbic acid (Sigma, St. Louis, MO),  $4 \times 10^{-4}$  M monothioglycerol (MTG, Sigma, St. Louis, MO), 100  $\mu\text{g/ml}$  Primocin (Invivogen, San Diego, CA), 2 mM L-glutamine (Invitrogen, Carlsbad, CA), 2 U/ml EPOgen (Amgen, Thousand Oaks, CA), 1% B-27 supplement (Thermo Fisher, Waltham, MA), 0.5% N-2 supplement (Thermo Fisher, Waltham, MA), 0.5% bovine serum albumin (BSA, Sigma, St. Louis, MO)] to generate more developmentally advanced erythroid-lineage cells.

For iPS-HSPCs generation, key changes were made to certain stages of the iPS-MEP protocol. In summary, dissociated hiPS colonies were plated onto matrigel-coated wells and hematopoietic differentiation was initiated once the cultures reached 10%–15% confluency (approximately 1–2 days). For both the iEry and iHSPC differentiation protocols, we found optimal hematopoietic differentiations are achieved with 10%–15% confluent hiPSC cultures comprised of evenly spaced small clusters of cells which allows sufficient space for the growth and establishment of the critical precursor mesodermal and endothelial cells before hematopoietic cell generation. Between D0 and D1 (2 days), cells were cultured with RPMI-1640 (Thermo Fisher, Waltham, MA), 10% KO serum replacement (KOSR; Thermo Fisher, Waltham, MA, #10828028), 50 ng/ml human vascular endothelial growth

factor A (hVEGFA), 5 ng/ml human bone morphogenic protein 4 (hBMP4), and 25 ng/ml hWnt3a. At D2: RPMI-1640, 10% KOSR, 50 ng/ml hVEGFA, 5 ng/ml hBMP4, 20 ng/ml human basic fibroblast growth factor (hbFGF), 3  $\mu\text{M}$  CHIR99021 (Tocris, Bristol, UK, #4423). At D3: StemPro-34 SFM (Thermo Fisher, Waltham, MA, #10639011), 50 ng/ml hVEGFA, 5 ng/ml hBMP4, 20 ng/ml hbFGF. Between D4 and D5: SP-34 serum free medium (SFM), 15 ng/ml hVEGFA, 5 ng/ml hbFGF. From D6 onwards, cells were continually cultured in HSPC medium, which is comprised of SP-34 SFM, 50 ng/ml hVEGFA, 100 ng/ml hbFGF, 100 ng/ml hSCF, 100 ng/ml hFLT3L, 100 ng/ml hTPO (Genentech, San Francisco, CA), 100 ng/ml human interleukin 6 (cytokines from R&D Systems, Minneapolis, MN). Fresh HSPC medium was added to the cultures every 1–2 days without aspiration of existing media. All culture media mixes contained 2 mM L-glutamine, 50  $\mu\text{g/ml}$  ascorbic acid,  $4 \times 10^{-4}$  M MTG, and 100  $\mu\text{g/ml}$  Primocin, and were cultured at 37°C in normoxic, 5% CO<sub>2</sub> conditions.

For experiments involving SB (activin/TGF $\beta$  inhibition), gamma secretase inhibitor (GSI; Notch inhibition), CH (AHR inhibition), and 6-formylindolo[3,2-b]carbazole (FICZ) (AHR activation); SB was added to D2 media (5.4  $\mu\text{M}$  SB-431542, Tocris, Bristol, UK), GSI was added to D4–5 and/or HSPC media (10  $\mu\text{M}$  L-685,458; Tocris, Bristol, UK), and CH and FICZ were added to D4–5 and/or HSPC media (10  $\mu\text{M}$  CH-223191, Tocris, Bristol, UK/0.2  $\mu\text{M}$  6-formylindolo[3,2-b]carbazole, Cayman Chemical, Ann Arbor, MI). In general, for all noted iHSPC culture conditions, we begin with  $0.5\text{--}1 \times 10^5$  hiPSCs (10% confluency), per well of a six-well plate, from which we eventually obtain  $2\text{--}4 \times 10^5$  floating hematopoietic progenitor cells by D15–16 of culture.

### Methycellulose Colony Assays

To assess hematopoietic colony forming unit (CFU) potential,  $2 \times 10^4$  to  $1 \times 10^5$  viable cells were plated in individual 35 mm dishes (StemCell Tech., Vancouver, CA; #27150) in 1.5 ml multi-lineage CFU semi-solid media (StemCell Technologies, Vancouver, CA; MethoCult H4034 Optimum) per dish. Duplicate dishes were generated for each condition. Colonies were scored after 14 days of culture at 37°C in normoxic, 5% CO<sub>2</sub> conditions. CFU values were normalized to the number of cells plated (CFU per  $10^4$  cells plated).

### MACs Separation

Isolation of CD34-enriched/depleted subpopulations was carried out with the MACs CD34 MicroBead Kit (human cells, Miltenyi Biotec, Bergisch, Germany; #130-046-702). Cells were either collected for RNA, put into CFU assays, or for adherent progenitor cells; replated onto matrigel-coated wells in HSPC medium.

### RNA Extraction and qPCR

RNA was extracted using the RNeasy kit (Qiagen, Hilden, Germany) according to manufacturer's recommendations and quantified using a NanoDrop Lite Spectrophotometer (Thermo Scientific, Waltham, MA). Up to 1000ng of RNA/sample was DNase-treated to remove trace contaminating genomic DNA using a DNA-free kit (Thermo Fisher, Waltham, MA). cDNA was generated using the High Capacity cDNA reverse Transcription Kit (Applied Biosystems, Foster City, CA) following manufacturer instructions. Diluted cDNA was used for quantitative polymerase

chain reaction (qPCR) analyses; predesigned TaqMan primers (Applied Biosystems, Foster City, CA) were used in conjunction with Taqman Universal Master Mix II (Applied Biosystems, Foster City, CA, #4440038) and the StepOne/QuantStudio 6 Flex Real Time PCR Systems (Applied Biosystems, Foster City, CA) following manufacturer's recommendations. Transcript levels were calculated using the relative standard curve method, normalized to the housekeeping gene beta actin.

### Western Blot for Globin Analyses

Cell pellets were resuspended in Roche lysis buffer (protease inhibitor, 0.3% NP-40 (Sigma, St. Louis, MO), 10% glycerine, 2 mM EDTA, 246 mM NaCl, 10% phosphatase inhibitor, phosphate-buffered saline [PBS], and water), placed on ice for 1 hour and centrifuged at 14,500 rpm for 15 minutes at 4°C to extract protein. Standard methodology was used for Western blot analysis. The following antibodies were used: HBB (16216-1-AP, Proteintech, Rosemont, IL), HBA (sc-21756, Santa Cruz Biotechnology, Dallas, TX), and GAPDH (sc-47724, Santa Cruz Biotechnology, Dallas, TX).

### Fluorescence-Activated Cell Sorting Analysis

Adherent cells were washed with Dulbecco's PBS (DPBS) (Thermo Fisher, Waltham, MA, #12563011) and treated with Tryp-LE Select (Thermo Fisher, Waltham, MA, #12563011) at 37°C for 5 minutes, followed by gentle pipetting to complete cell dissociation. The dissociated cells were then washed with DPBS several times before antibody staining for flow cytometry. For suspension hematopoietic cells, gentle pipetting was used to dislodge any loosely adhered hematopoietic cells from the adherent stromal layer, and the cells were washed multiple times with PBS before staining. Cells were stained in ice-cold fluorescence-activated cell sorting buffer (PBS, 1% BSA). Antibodies used; KDR-PE (BD Pharmingen, San Jose, CA, #560872), CD34-APC (BD, San Jose, CA, #555824), CD144-PE (BD, San Jose, CA, #561714), CD45-PE (BD, San Jose, CA, #561866), CD117-APC (Thermo Fisher, Waltham, MA, clone 104D2), CD117-PE (BD, San Jose, CA, #555714), CD235a-FITC/PE (BD, San Jose, CA, Clone GA-R2 (HIR2)), CD41a-APC (BD, San Jose, CA, #559777), CD71-FITC (BD, San Jose, CA, #555536), CD73-PE (BD, San Jose, CA, #561014), CXCR4-Biotin (BD, San Jose, CA, #555973), and Streptavidin-FITC (BD, San Jose, CA, #554060). Flow cytometry was conducted on a Stratadigm S1000EXI or Beckton Dickinson (BD) dual-laser FacsCalibur flow cytometer. Analyses were conducted using FlowJo v8.7 (FlowJo, LLC) software.

### BrdU Assay

Cell cycle analysis of iPS-HSPCs was carried out using the FITC BRDU Flow Kit (BD Pharmingen, San Jose, CA) following manufacturer's recommendations. 5'-Bromo-2'-deoxyuridine (BrdU) substrate was added to iPS-HSPC cultures 18 hours before collection for analyses; samples were prestained with mouse anti-human CD34-APC (BD; San Jose, CA, #555824) before fixation.

**DGE Analysis.** For digital gene expression (DGE), RNA was collected from all samples using the RNeasy Mini Kit (Qiagen, Hilden, Germany) and sent out for library construction and sequencing at the Broad Institute (Cacchiarelli, Trapnell et al. 2015). Samples were rescaled to a common target across plates and cubic root transformed to follow approximately normal

distribution. Differential expression was tested using *t*-tests and level of significance was corrected using Bonferroni correction. Data are displayed using heatmaps generated with the Heatplus package in R v3. Enrichment analysis was conducted using the David portal (<https://david.ncicrf.gov/home.jsp>).

**3C Assay.** Approximately  $2 \times 10^6$  iPS-derived erythroid progenitor (iEry or iHSPC-Ery) cells were harvested after 25 days differentiation and crosslinked with 1% formaldehyde for 10 minutes at room temperature, followed by glycine quenching at a final concentration of 125 mM. Crosslinked cells were lysed with ice cold lysis buffer (10 mM Tris-HCl at pH 8.0, 10 mM NaCl, 5 mM MgCl<sub>2</sub>; 0.2% NP-40, 1× complete protease inhibitor) for 10 minutes and nuclei were harvested. The nuclei were resuspended in nuclei lysis buffer and incubated for 1 hour at 37°C with vigorous shaking. Triton X-100 was added to 2% to sequester the SDS, and the samples were incubated for 1 hour at 37°C. Samples were further digested with EcoRI (New England Biolabs, Ipswich, MA) overnight at 37°C, and intramolecularly ligated with T4 ligases (New England Biolabs) for 4.5 hours at 16°C and 30 minutes at room temperature. Digestion and ligation efficiencies were monitored. Samples were further reverse crosslinked overnight at 65°C and DNA from a chromatin conformation capture (3C) library was then purified by phenol extraction and ethanol precipitation. A template titration of the 3C library was performed to generate the linear range of amplification. 3C ligation products were quantified in triplicates by real-time using SYBR Green real-time qPCR (Applied Biosystems 7500 Real-Time PCR System).

## RESULTS

### Generation and Characterization of iPS-Derived HSPC-Like Cells

We have described previously the efficient derivation of large numbers of MEP cells from a monolayer hPSC differentiation protocol [32]. In this system, suspension cells that emerge from an adherent layer of endothelial and stromal cells are comprised of bipotent CD235a<sup>+</sup>CD41a<sup>+</sup> progenitor cells that upon further specification, can generate low ploidy, platelet-producing megakaryocytes, and hemoglobinized erythroblasts with primitive and fetal characteristics. The abundance of embryonic and fetal globins coupled with a lack of adult globin in these erythroblasts suggested that these differentiation conditions favor the formation of predominantly embryonic-type (yolk sac) erythroblasts.

Here, we have modified our differentiation protocol to define a set of conditions that allows for the robust, experimentally reproducible, specification, and expansion of populations of definitive-lineage hematopoietic stem progenitor-like cells (HSPCs) from which adult-type blood cells can be derived. This differentiation protocol (iPS-HSPC) retains the advantages of the previously described iPS-MEP system in that it is also monolayer, serum-free, and augmented by the temporal control of signaling pathways through stage-specific cytokine modulation (Fig. 1A). Cell formation is clearly visible in this culture system as an immediate read-out of the efficiency of hematopoiesis under defined conditions (Fig. 1D). In HSPC media, emerging hematopoietic cells, generated through the process of EHT, can be observed from approximately D8+

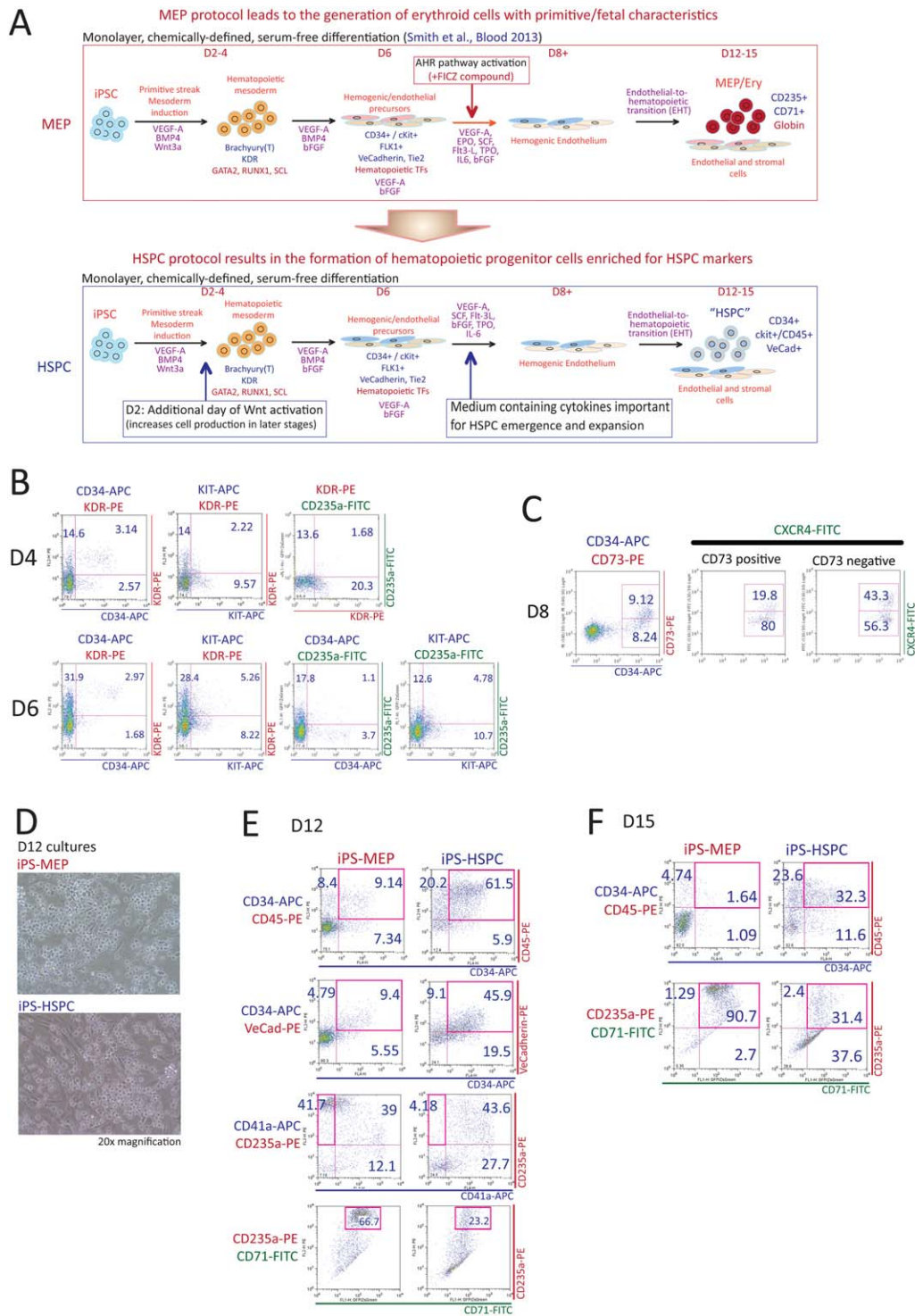


**Figure 1.** Characterization of the induced pluripotent stem (iPS)–hematopoietic stem-progenitor cell (HSPC) differentiation protocol. **(A):** Schematic representation highlighting the differences between the iPS-megakaryocyte–erythroid progenitor (MEP) versus the iPS-HSPC differentiation protocols. **(B):** Representative fluorescence-activated cell sorting (FACS) analyses of early hem–endothelial cell surface markers. **(C):** Representative FACS analyses of arterial/venous/hemogenic endothelial cell populations. D8 adherent cells were analyzed for CD34, CD73 and CXCR4 expression. **(D):** Photomicrographs of D12 iPS-MEP and iPS-HSPC cultures. Suspension hematopoietic cells can be observed floating above the adherent cell layer. **(E):** Representative FACS analyses of D12 iPS-MEP and iPS-HSPC suspension cells for early/widely expressed hematopoietic cell surface markers (CD34, CD45, VeC and CD41a) and erythroid specific markers (CD235a, CD71). **(F):** Representative FACS analyses of D15 iPS-MEP and iPS-HSPC suspension cells for early (CD34, CD45) and erythroid specific markers (CD235a, CD71). Abbreviations: AHR, aryl hydrocarbon receptor; bFGF, basic fibroblast growth factor; BMP, bone morphogenic protein; EHT, endothelial-to-hematopoietic transition; EPO, erythropoietin; FICZ, 6-formylindolo[3,2-b]carbazole; HSPC, hematopoietic stem-progenitor cell; IL6, interleukin 6; iPSC, induced pluripotent stem cell; MEP, megakaryocyte–erythroid progenitor; RUNX1, SCF, stem cell factor; TPO, thrombopoietin; VEGF, vascular endothelial growth factor.

of culture, and steadily expand in number as the culture progresses (Supporting Information Movie S1).

The first definitive lineage hematopoietic progenitor cells that arise *in vivo* in the AGM can be identified by coexpression of the pan-endothelial/hematopoietic cell surface markers CD34, CD45, Ve-Cadherin (CD144), and cKIT (CD117) [43]. In our system, modeling early hematopoietic development, hematopoietic/endothelial mesodermal cell populations are observed in the culture between D4 and D6; at this timepoint, KDR<sup>+</sup>CD34<sup>+</sup> and CD235a<sup>+</sup> cells represent subsets of mesodermal cells fated to generate endothelial cells (including definitive hemogenic endothelium) and primitive Erys, respectively [7] (Fig. 1B). By D8, as the process of hematopoietic cell emergence begins, the CD34<sup>+</sup> cells of the adherent cell population can be fractionated into CD34<sup>+</sup>CD73<sup>+</sup>CXCR4<sup>-</sup> (hemogenic endothelium), CD34<sup>+</sup>CD73<sup>+</sup>CXCR4<sup>-</sup> (venous) and CD34<sup>+</sup>CD73<sup>+</sup>CXCR4<sup>+</sup> (arterial) subsets [44] (Fig. 1C). CD73 and CXCR4 are not expressed at earlier timepoints (Supporting Information Fig. S1A). Fractionation of D6 and D8 cultures based on CD34 expression and extended culture of these cells confirmed that the vast majority of endothelial and hematopoietic potential resides within the CD34<sup>+</sup> cell population at these timepoints (Supporting Information Fig. S1B, S1C).

As round, hematopoietic suspension cells begin to emerge in our iPS-HSPC system, and in contrast to the iPS-MEP protocol, iPS-HSPC cultures are greatly enriched for both CD34<sup>+</sup>CD45<sup>+</sup> and CD34<sup>+</sup>VeC<sup>+</sup> cells, suggesting that these conditions favor the emergence, expansion, and maintenance of putative HSPCs (Fig. 1E). Additionally, when comparing the two protocols, there is also a striking decrease in the number of erythroid-committed cells (CD235a<sup>+</sup>/CD235a<sup>+</sup>CD71<sup>+</sup>) in iPS-HSPC cultures (Fig. 1E, 1F). As the differentiation progresses, the number of iPS-HSPC suspension hematopoietic cells robustly increases in number. By D15–D16, the yield is in the range of 2–4 × 10<sup>5</sup> suspension cells per well of a six-well plate, originally seeded with hiPS at 10%–15% confluency (Supporting Information Fig. S1D). The proportion of CD34<sup>+</sup>/CD45<sup>+</sup> cells gradually decreases as the differentiation progresses after D12 but constitutes approximately 20%–40% of the suspension hematopoietic cells at D15–16. Approximately 20%–40% of D15–16 cells are positive for CD34/CD45 which represent more mature, non-erythroid committed hematopoietic cells. In contrast, at this timepoint, the vast majority of suspension cells in iPS-MEP cultures are negative for CD34/CD45 and are erythroid-committed (CD235a<sup>+</sup>CD71<sup>+</sup>) (Fig. 1F). Notably, similar patterns of iPS-HSPC emergence, expansion, and cell surface marker distributions were observed for multiple hiPSC lines, including wild-type (WT) and blood disease-specific lines (data not shown).

### Modulation of ActivinA/TGFβ/Nodal and Wnt Pathways in the Production of iPSC-Derived HSPCs

Studies on the modulation of key tissue-patterning signaling pathways in a hPSC EB model for hematopoietic differentiation suggest that early-stage inhibition and activation of ActivinA/TGFβ/Nodal and Wnt pathways, respectively, skew differentiation outcomes toward definitive rather than primitive hematopoietic cells [7, 8, 45]. In our differentiation system, the formation of primitive streak and resultant hematopoietic mesoderm occurs in the D2–6 timeframe, as determined by time course expression of Brachyury (T) and GATA2 (data not

shown) and cell surface expression of KDR, CD34 and CD235a (Fig. 1B). We tested the effects of the ActivinA/TGFβ/Nodal inhibitor SB-431542 (SB) and the Wnt agonist/GSK3 inhibitor CHIR99021 (CHIR) on the specification of hematopoietic endothelial cells when added at early stages of the iPS-HSPC differentiation system (Supporting Information Fig. S2A). Adherent cells at D6 of differentiation, consisting of pre-EHT hematopoietic mesodermal/endothelial progenitor cells, were analyzed for the cell surface expression of endothelial/early hematopoietic markers CD34, CD235a, Ve-Cadherin, and cKit by flow cytometry. CD235a<sup>+</sup> cells at this stage in development are fated to form primitive hematopoietic progenitor cells. There was a striking decrease in the population of CD235a<sup>+</sup> cells in D3-SB treated cultures, in agreement with the observation that CD235a<sup>+</sup> cells at this developmental timepoint are fated to form primitive hematopoietic progenitor cells and that early-stage ActivinA/TGFβ inhibition results in a block in primitive hematopoietic potential [7]. SB treatment also led to an approximately 10-fold increase in the proportion of CD34<sup>+</sup> cells, and an increase in the number of VeC<sup>+</sup> cells. Treatment with CHIR (D2) did not have an effect on CD235a, CD34, or VeC expression in D6 cultures, but numbers of cKIT<sup>+</sup> cells were markedly increased (Supporting Information Fig. S2B).

Notably, our analyses of later-stage iPS-HSPC cultures revealed differences in the proportions of hematopoietic cells generated upon early SB and CHIR treatment, with SB-treated cultures giving rise to far fewer suspension hematopoietic progenitor cells. Conversely, CHIR-treated cultures were robust and gave rise to comparable numbers of cells as control cultures. Of the cells that were generated, the proportion of CD34<sup>+</sup>CD45<sup>+</sup> cells was broadly similar for SB- and CHIR-treated cultures (Supporting Information Fig. S2C). However, D2 + SB suspension cells demonstrated markedly decreased multi-lineage hematopoietic potential in CFU assays (Supporting Information Fig. S2D). In contrast, CHIR cultures gave rise to hematopoietic progenitor cells that had similar CFU potential to control cultures. As SB treatment produced fewer overall cells and had a negative end-stage impact on iPS-HSPC formation and functionality, we no longer include this small molecule in our iPS-HSPC culture conditions. Although additional Wnt signaling via CHIR is not always necessary to drive definitive hematopoiesis from hPSCs as some hPSC lines generate sufficient endogenous Wnt signaling, CHIR is included in our iPS-HSPC differentiation protocol to normalize definitive pathway potential across multiple hiPSC lines.

### iPS-HSPCs Are Enriched for Hematopoietic Colony-Forming Potential as Compared with iPS-MEP Cells

To ascertain the hematopoietic potential of iPS-HSPCs at different timepoints, D12 and D16 unfractionated suspension cells were plated in multi-lineage CFU assays along with timepoint-matched iPS-MEP cells. While D12 iPS-HSPCs produced limited numbers of small red cell clusters that match the morphology of primitive erythroid colonies (Fig. 2A), D16 iPS-HSPC cultures were able to give rise to abundant erythroid (BFU and CFU-erythroid) colonies (Fig. 2B, 2C). There was a notable difference in the erythroid potential of iPS-HSPCs at the different timepoints; D12 cells gave rise to limited numbers of small red cell clusters that were similar to the morphology of primitive erythroid colonies (Fig. 2A), while D16 iPS-HSPC cultures were able to give rise to abundant

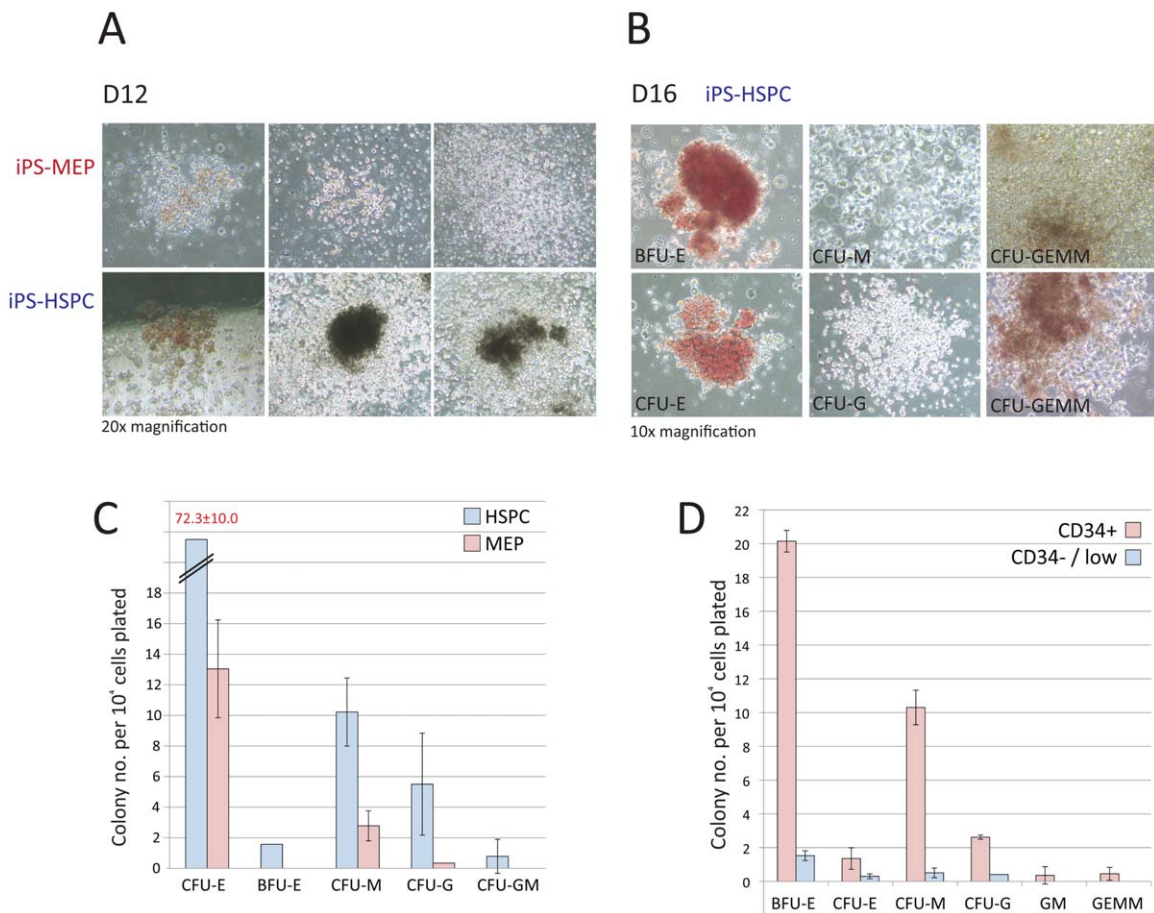


**Figure 2.** The induced pluripotent stem (iPS)–hematopoietic stem-progenitor cell (HSPC) protocol results in the robust production of functional hematopoietic progenitor cells. **(A):** Photomicrographs of hematopoietic colonies formed by D12 iPS-megakaryocyte–erythroid progenitor (MEP) and iPS-HSPC suspension cells. **(B):** D16 iPS-HSPC cultures are able to robustly generate erythroid and myeloid (macrophage, granulocyte, granulocyte–macrophage) colonies. **(C):** Comparison of multi-lineage colony forming unit (CFU) potential of D16 iPS-HSPC versus iPS-MEP cultures. Representative results from three independent experiments. Error bars = SD. **(D):** Quantification of CFU potential in CD34<sup>+</sup>/low and CD34<sup>+</sup> cells in D16 iPS-HSPC cultures. Representative results from three independent experiments. Error bars = SD. Abbreviations: BFU, burst forming unit; CFU, colony forming unit; E, erythroid; G, granulocyte; GEMM, granulocyte erythroid macrophage megakaryocyte; GM, granulocyte–macrophage; HSPC, hematopoietic stem-progenitor cell; iPS, induced pluripotent stem cell; M, macrophage; MEP, megakaryocyte–erythroid progenitor.

large erythroid (BFU and CFU-erythroid) colonies (Fig. 2B, 2C). This suggests that BFU/CFU-e cells are only present in later-staged iPS-HSPC cultures. Myeloid (granulocyte, macrophage, and granulocyte–macrophage; G, M, GM, respectively) colonies were observed in both D12 and D16 iPS-HSPC CFU cultures. In contrast, iPS-MEP cultures displayed comparatively poor colony forming potential at both timepoints, although single Erys and small Ery colonies were visible.

CD34<sup>+</sup>CD45<sup>+</sup> cells represent a significant proportion of the suspension cells generated in our iPS-HSPC cultures by D12–16, and CD34<sup>+</sup> hematopoietic cells have been shown to be enriched for stem/progenitor functionality [43, 46, 47]. To assay the functional characteristics of the CD34<sup>+</sup> iPS-HSPCs, D15 CD34<sup>+</sup> cells were enriched by MACs magnetic bead selection. The resulting CD34-enriched (ENR; CD34<sup>+</sup>) and depleted (CD34-/low) cells were plated in multi-lineage methylcellulose to ascertain CFU potential. In these assays, CD34<sup>+</sup> cells were able to give rise to many more erythroid [both blast (BFU-E) and colony forming (CFU-E)] units and myeloid colonies (CFU-G, GM, and M) compared with the CD34-/low

population (Fig. 2D). These results indicate that the majority of the colony forming activity in iPS-HSPC cultures resides within the CD34<sup>+</sup> cells present within the culture.

#### Global Comparative Gene Expression Analysis of CD34<sup>+</sup> iPS-HSPCs versus Primary Fetal and Adult CD34<sup>+</sup> Hematopoietic Progenitor Cells

We compared the global transcriptomic profile of CD34<sup>+</sup> iPS-HSPCs with CD34<sup>+</sup> FL and adult BM cells using DGE analysis. RNA was extracted from MACs-purified CD34<sup>+</sup> iPS-HSPCs at D13, D15, and D16 of culture and compared with RNA from CD34<sup>+</sup> FL hematopoietic cells and CD34<sup>+</sup> adult BM cells. Unsupervised clustering of the samples revealed that the primary CD34<sup>+</sup> FL and CD34<sup>+</sup> BM samples were transcriptionally similar, with a clear fetal versus adult-type signature (Supporting Information Fig. S3A). CD34<sup>+</sup> iPS-derived cells display a transcriptionally distinct signature when compared with the primary samples, with D13 iPS-derived CD34<sup>+</sup> cells closest to the native samples, as judged by fewer differentially regulated genes (Supporting Information Fig. S3A). Overall, there were 57 significantly

differentially regulated genes between FL and BM CD34<sup>+</sup> cells ( $p \leq .05$ , FDR  $\leq .05$ ), while D13 iPS-HSPCs had 1,192 and 1,357 differentially expressed genes compared with FL and BM CD34<sup>+</sup> cells, respectively (Supporting Information Fig. S3B).

Using Panther (<http://pantherdb.org/>), the lists of differentially expressed genes were examined to identify key biological processes and signaling pathways that differ between the sample sets. As other studies have identified a paucity of Notch signaling pathway genes in mESC-derived hematopoietic cells compared with *in vivo* HSCs, we were interested to see whether this would also be the case in iPS-HSPCs compared with FL and BM cells. Many genes related to Notch signaling were not significantly differentially regulated in iPS-HSPCs compared with FL cells, but levels of Notch2 and Hes6 transcripts were significantly lower compared with BM cells, suggesting that overall Notch signaling activity is comparable between iPS-HSPCs and FL cells, and perhaps BM cells. Notch1, Notch ligands such as DLL4 and JAG1, and important downstream target genes for hematopoiesis were not differentially regulated when comparing primary cells with iPSC-derived cells (Supporting Information Fig. S3C, S3D, Panther gene lists not shown). As the DGE analyses used RNA from cell populations, it is not possible to ascertain from this data whether there are rare CD34<sup>+</sup> cell populations in the iPS-HSPCs that may display gene expression patterns more aligned with the patterns observed in fetal and adult CD34<sup>+</sup> hematopoietic progenitor cells.

### Developmentally Patterned HSPCs Can Produce Erythroblasts with Adult-Type Characteristics

iPS-HSPCs are capable of efficient CFU-e and BFU-e formation in multi-lineage CFU assays (Fig. 3A) and although the vast majority remain nucleated, they appear morphologically similar in size to human peripheral blood erythrocytes when compared with iPS-MEP-derived cells (Fig. 3B). To assess the transcriptional expression of globin species present, iPS-HSPC erythroid colonies were isolated and compared with erythroblasts generated via the iPS-MEP method by qPCR. iPS-HSPC-derived Erys (iHSPC-Ery) express 2–3 log-fold more  $\beta$ -globin when compared with iPS-MEP-derived erythroblasts (iEry), but do not achieve the levels observed in peripheral blood mononuclear cell-derived Erys (pbMNC-Ery) (Fig. 3C). While embryonic and fetal globins are still expressed in iHSPC-Ery cells, the expression levels are significantly less than that of iEry cells, suggesting that although the degree of maturational globin switching is incomplete within the iHSPC-Ery population as a whole, it is more advanced than that found in iEry cells. These patterns of differential globin gene expression were confirmed by DGE analysis which also allowed for global transcriptomic mapping of the differences between iHSPC-Ery cells, iEry cells, and primary erythroblast counterparts (CD34<sup>+</sup> mobilized peripheral blood cells differentiated into nucleated erythroid-lineage cells were used for this experiment as enucleated, end-stage erythrocytes lack sufficient RNA content). Confirming the qPCR analyses,  $\beta$ -globin gene expression was higher in iHSPC-Ery cells compared with iEry cells, although lower than in primary CD34<sup>+</sup>-Ery cells. HBD/ $\delta$ -globin was also upregulated in iHSPC-Ery cells;  $\delta$ -globin is also restricted to adult Erys, and together with  $\alpha$ -globin (HbA<sub>2</sub> $\alpha$ 2 $\delta$ 2) constitutes about 2.5% of total adult Hb. In contrast to these results, the levels of  $\zeta$  (HBZ, embryonic  $\alpha$ -like globin),  $\gamma$  and  $\epsilon$  globin

species were lower in iHSPC-Ery cells compared with iEry cells, again suggesting that iHSPC-Ery cells are more functionally mature than cells produced via the primitive pathway. Notably, the expression of *KLF1* and *BCL11A*, two transcription factors known to be important for the silencing of *HBB* and the upregulation of  $\beta$ -globin [48–50], was increased in iHSPC-Ery cells (Fig. 3D, additional data in Supporting Information Fig. S4).

Next, to examine protein-level production of  $\gamma$  and  $\beta$  globins in iEry cells when compared with iHSPC-Ery cells, Western blotting was performed on both WT and SCD-specific iPSC-derived cells (Fig. 3E). As controls for these experiments, the HUDEP-1 and 2 erythroblast cell lines [51] were used which predominately express either  $\gamma$  or  $\beta$  globin, respectively. As predicted by the transcriptional data, iHSPC-Ery cells produce significantly more  $\beta$  globin at the protein level than their iEry counterparts produced from the same parental lines (Fig. 3E). Although a faint band appears in iEry cells in the  $\beta$  globin Western analysis, this band appears at a significantly different molecular weight suggesting nonspecific antibody binding or the production an alternate  $\beta$ -globin moiety in iEry cells.

Finally, to interrogate potential chromatin landscape differences between iEry and iHSPC-Ery cells, 3C assays were performed (Fig. 3F). Results from these assays demonstrated that iHSPC-Ery cells have increased LCR (HS432) looping to the *HBB* promoter compared with iEry cells. Notably, the interaction frequency between the LCR and the *HBB* promoter is increased 2.6-fold in iHSPC-Ery cells ( $p < .05$ ). We also detected a decrease in the interaction frequency between the LCR and *HBB* promoter in iHSPC-Ery cells versus in iEry cells. These results are consistent with our finding that *HBB* gene expression is increased in iHSPC-Ery cells compared with iEry cells, and suggests that LCR looping to the *HBB* promoter is one of the mechanisms by which *HBB* gene expression is unregulated in iHSPC-Ery cells.

### Notch Signaling Is Required During Hematopoietic Mesoderm Development, in the Formation of iPS-HSPCs, and in the Production of Resultant Erythroid Progeny

The Notch signaling pathway is a prerequisite for the formation of definitive-lineage hematopoietic cells *in vivo* [25, 52] and also for vascular morphogenesis and arterial/venous fate specification of vessels [53–55]. It is, however, dispensable for the formation of primitive yolk sac hematopoiesis. As such, it is one of the key molecular pathways that differentiates between the primitive and definitive branches of the hematopoietic system. To ascertain whether the emergence of iPS-HSPCs is dependent on Notch signaling, we exposed hematopoietic cultures to 10  $\mu$ M GSI (a global Notch inhibitor) in a stage-specific manner to determine the effect on hematopoietic cell emergence and growth. Cultures were dosed between D4 and D5, from D6 onwards (D6+) or from D4 onwards (D4+), focusing on the key developmental timepoints corresponding to hematopoietic mesoderm and hemogenic endothelium generation (Fig. 4A). Statistically significant differences in cell number were noted in the control versus GSI-treated iPS-HSPC cultures, with far fewer suspension hematopoietic cells produced in cultures treated with GSI between D4 and D5 and D4+ (Fig. 4B, 4C). Interestingly, GSI treatment from D6+ appeared to have only a mild effect on hematopoietic cell output, suggesting that Notch signaling is not required at this later timepoint for hematopoietic cell emergence, which is



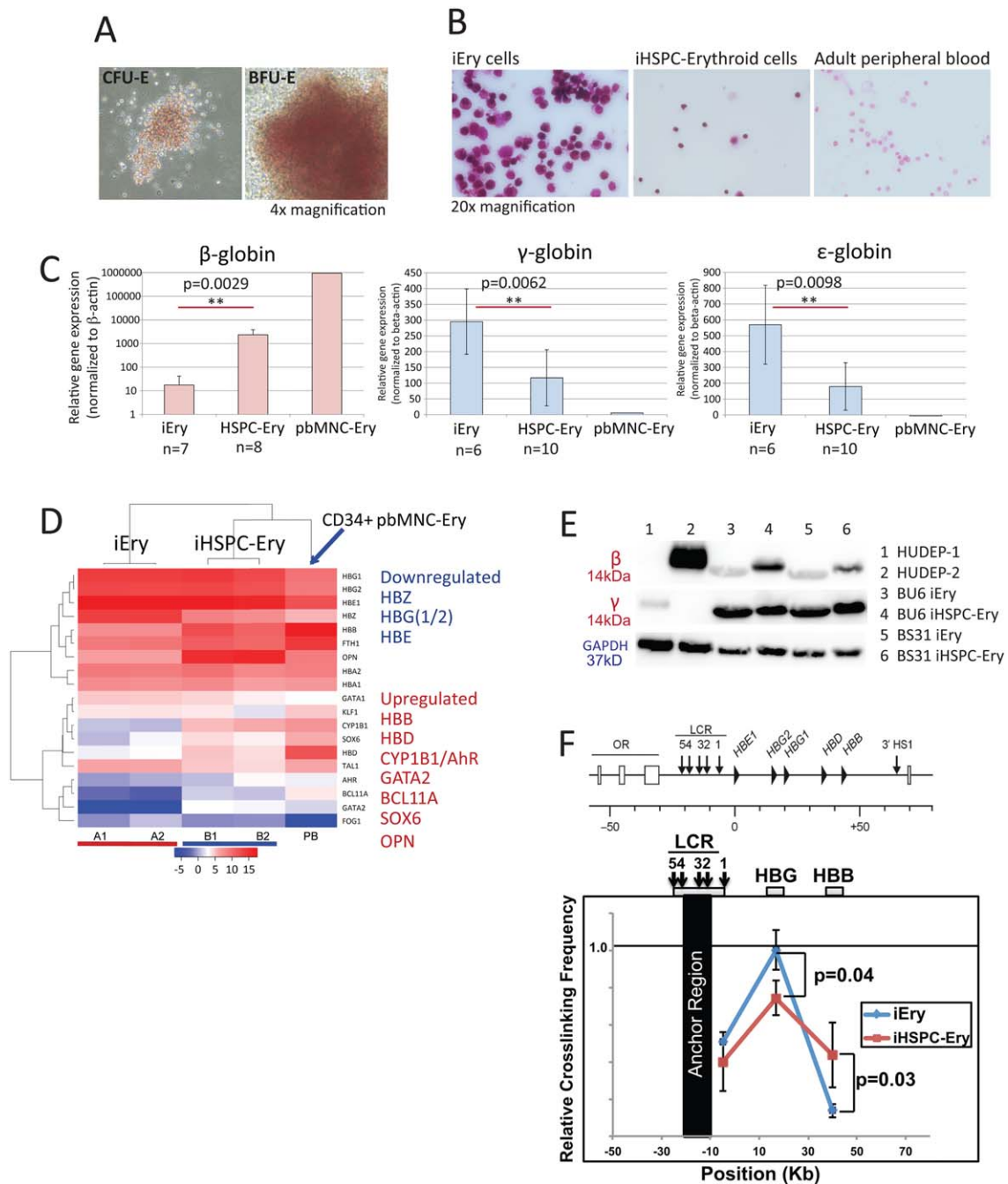


**Figure 3.** Induced pluripotent stem (iPS)-hematopoietic stem-progenitor cells (HSPCs) give rise to erythroid cells (Ery) with enhanced adult globin expression. **(A):** Photomicrographs of iPS-HSPC derived colony forming unit/BFU-erythroid colonies. **(B):** Photomicrographs of Wright-Giemsa-stained iPS-derived megakaryocyte-erythroid progenitor Erys (iEry) and HSPC-derived Erys (iHSPC-Ery) and human peripheral blood erythrocytes. **(C):** Quantitative gene expression analyses of globin expression levels of iHSPC-Ery compared with iEry and CD34<sup>+</sup> peripheral blood mononuclear blood cell-derived Erys (pbMNC-Ery). All values normalized to  $\beta$ -actin. Error bars = SD. **(D):** Heatmap of genes of interest relating to erythropoiesis, generated with digital gene expression sequencing data. Colors represent Log<sub>2</sub>-counts per million transcript levels. Two independent samples were analyzed for iEry and iHSPC-Ery sample types, with technical triplicates for each sample. **(E):** Western blot analysis of  $\gamma$  and  $\beta$  expression in iEry and iHSPC-Ery cells. (HUDEP 1 and 2: Postnatal erythroblast cell lines which express either  $\gamma$  or  $\beta$  globin, respectively; BU6: wild-type induced pluripotent stem cell [iPSC] line; BS31: SCD-specific iPSC line). **(F):** LCR looping to the *HBG* or *HBB* promoter in iEry or iHSPC-Ery iPSC-derived erythroid progenitor cells. Chromatin conformation capture (3C) assay measuring crosslinking frequencies between the LCR and *HBG* or *HBB* promoters in iEry or iHSPC-Ery cells. The EcoR1 fragment containing HS432 of the LCR (black bar) was used as the anchor region. Its crosslinking frequency with EcoR1 fragments that contain *HBG* or *HBB* or *HS1* was assessed. The interaction between fragments within the  $\alpha$ -tubulin gene was used as the internal normalization control for 3C signals, and the highest cross-linking frequency value was set to one. Spatial organization of the human  $\beta$ -globin locus is indicated at the top. The x-axis shows position (in kilobases) in the locus. All data are plotted as the mean SD of the measurement,  $p < 0.05$  ( $n = 3$ ). Abbreviations: BFU, burst forming unit; CFU, colony forming unit; E, erythroid; Ery, erythroid cell; HBB, hemoglobin comprised of beta; iHSPC, induced hematopoietic stem-progenitor cell; LCR, locus control region; pbMNC, peripheral blood mononuclear cell.

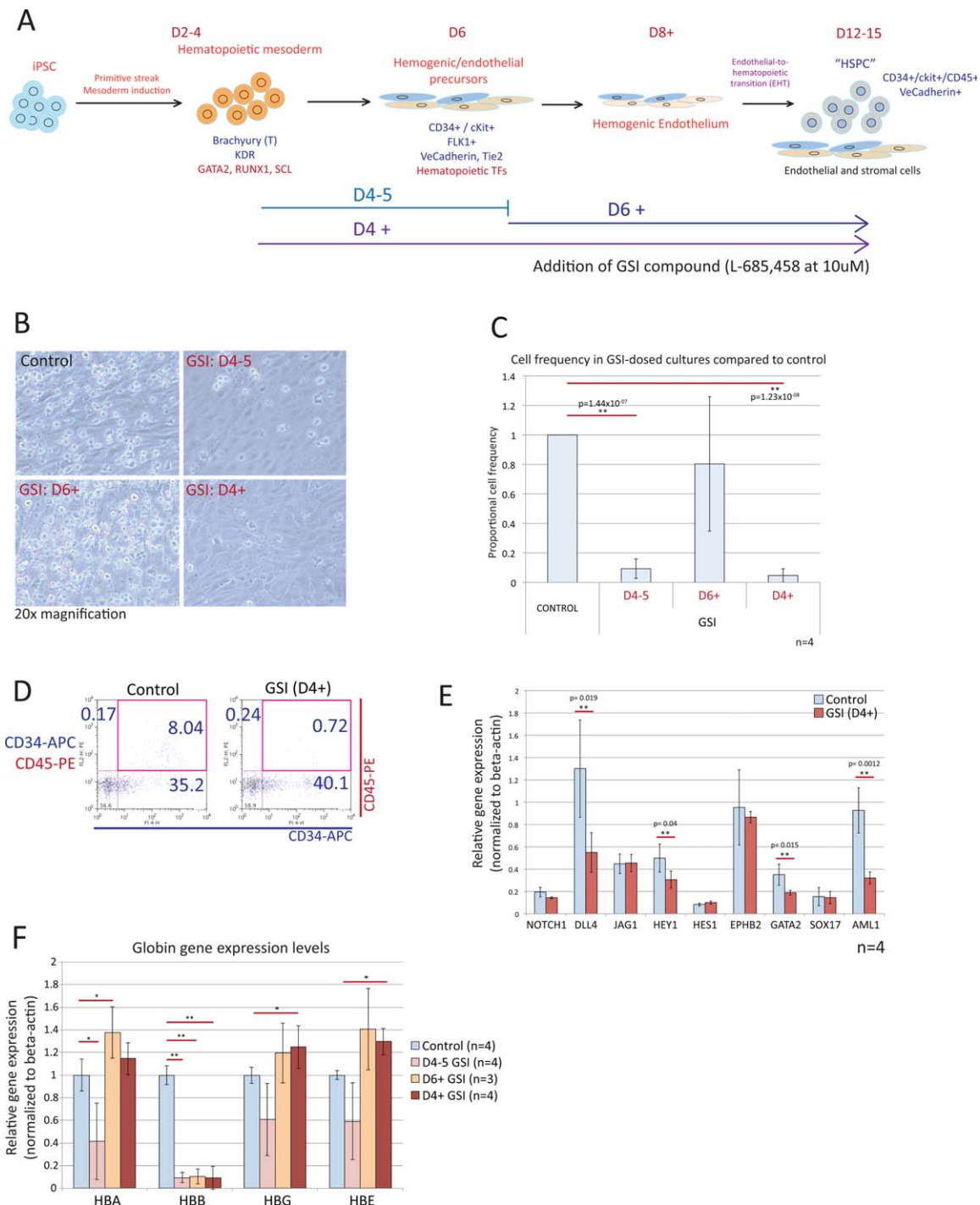


**Figure 4.** Hematopoietic progenitor cell formation in induced pluripotent stem (iPS)-hematopoietic stem-progenitor cell cultures is dependent on stage-specific notch signaling. **(A):** Schematic diagram illustrating gamma secretase inhibitor (GSI) dosing scheme. **(B):** Photomicrograph of D15 cell cultures. Cultures were treated with GSI at D4–5 or D4 onward (D4+) and display dramatically reduced hematopoietic cell emergence. **(C):** Quantification of D15 suspension hematopoietic cells generated in control/GSI-treated cultures; cell numbers were normalized to the control for each experimental set. Error bars = SD. Statistical significance determined by Student’s *t* test analysis. **(D):** Analysis of D10 control and GSI-treated cultures for CD34 and CD45 revealed intact endothelial cell formation (CD34<sup>+</sup>CD45<sup>-</sup>) but reduced hematopoietic cell formation (CD34<sup>+</sup>CD45<sup>+</sup>) in GSI-treated cultures. **(E):** Gene expression analyses of D10 control versus GSI-treated cultures for a panel of hematopoietic and signaling genes of interest. DLL4, HEY1, GATA2, and AML1 are significantly downregulated in GSI-treated cultures, as determined by Student’s *t* test analysis. All expression levels normalized to beta actin housekeeping gene. Error bars = SD. **(F):** Globin gene expression analyses of erythroid cells generated from control and stage-specific GSI-treated cultures. Error bars = SD. Statistical significance determined by Student’s *t* test analysis. Abbreviations: EHT, endothelial-to-hematopoietic transition; GATA2; GSI, gamma secretase inhibitor; HBA, hemoglobin comprised of alpha; HBB, hemoglobin comprised of beta; HBE, embryonic hemoglobin; HBG, hemoglobin comprised of gamma; HSPC, hematopoietic stem-progenitor cell; iPSC, induced pluripotent stem cell; RUNX1; SCL.

usually visible from D7 to D8 onwards. Notably, the impact of GSI-treatment on the adherent endothelial cell population was minimal with comparable percentages of CD34<sup>+</sup> cells present in control and D4+ GSI treated cultures at D10. However, a vast reduction in CD34<sup>+</sup>CD45<sup>+</sup> hematopoietic cells was seen in GSI-treated populations (Fig. 4D). Earlier endothelial cell compartments also appear to be unaffected in D4–5 GSI-treated cultures at D6 and D8 of development (Supporting Information Fig. S5). Analyses of D10-staged D4 + GSI-treated cultures for the gene expression of key hematopoietic and Notch pathway genes revealed a decrease in expression levels of *DLL4*, *HEY1*, *GATA2*, and *AML1*, while other notch pathway (*NOTCH1*, *JAG1*, and *HES1*) and known target genes (Ephrin B2; *EPHB2*, an arterial marker [55]) were unaffected (Fig. 4E). The downregulation of *AML1* may account for the vast reduction in hematopoietic cell formation in the GSI-treated cultures, as it is known to be important for EHT [56] and has been shown to be a Notch target in murine AGM tissues [57].

While the number of iPS-HSPCs was vastly reduced in D4–5/D4+ GSI-treated cultures, the cells that did emerge were able to form myeloid and erythroid colonies in multi-lineage CFC assays (data not shown). To gain a better understanding of exactly how primitive vs definitive potential is affected upon Notch inhibition, iPS-MEP differentiations (representing primitive wave hematopoietic cells with low-level adult globin expression) were carried out with control/stage-specific GSI-treated cultures to assess the impact of Notch inhibition on embryonic, fetal and adult globin expression in resultant Erys. Similarly to iPS-HSPC cultures, there was a decrease in hematopoietic cell emergence in cultures treated at D4–5/D4+, but Erys were successfully generated from cultures under all conditions. Strikingly, the Erys generated from all GSI-treated cultures expressed greatly reduced levels of  $\beta$ -globin compared with control cultures, while levels of  $\alpha$ -,  $\epsilon$ -, and  $\gamma$ -globin were similar across all sample types (Fig. 4F). The detrimental effect of Notch inhibition on  $\beta$ -globin expression in this system reveals a requirement for Notch signaling during both early hematopoietic mesoderm and hemogenic endothelium formation as well as for the generation of adult-type Erys that are able to express  $\beta$ -globin.

### AHR Signaling Plays a Stage-Specific Role in Developmental Hematopoiesis

AHR modulation can be used to expand and maintain primary HSPC populations [36, 37], and AHR signaling may also play a role in the generation of early hematopoietic progenitor cells from hPSCs [39, 40] (p171)]. In these studies, we used our iPS-HSPC system to examine the role of AHR signaling in developmental hematopoiesis.

To assess the function of AHR in developmental hematopoiesis in the context of the iPS-HSPC model, genetic ablation and small molecule modulation of AHR expression were used as outlined in Figure 5A. First, CRISPR-Cas9 gene editing was used to create homozygous AHR KO lines from multiple parental hiPSCs, resulting in a lack of AHR protein production and functional activity in undifferentiated iPSCs and their resultant progeny (Supporting Information Fig. S6A, S6B). iPS-HSPC differentiations of these lines revealed a twofold increase in emergent hematopoietic cells in AHR<sup>-/-</sup> cultures compared with WT (Fig. 5B; Supporting Information Fig. S6C). In addition to increased hematopoietic cell production, analyses of D15 AHR<sup>-/-</sup>

cells for cell-surface hematopoietic markers revealed an approximately twofold increase in the proportion of CD34<sup>+</sup>CD45<sup>+</sup> cells present in the culture compared with WT cultures, suggesting an increase in HSPC-like cells. (Fig. 5C; Supporting Information Fig. S6D). Interestingly, fewer AHR<sup>-/-</sup> iPS-HSPCs were cKIT/CD117<sup>+</sup> compared with WT cells (Fig. 5C). D15 AHR<sup>-/-</sup> iPS-HSPCs were also plated in multi-lineage CFU assays to ascertain the hematopoietic potential of the AHR<sup>-/-</sup> cells compared with WT. Notably, in comparison with WT, AHR<sup>-/-</sup> cells gave rise to significantly more myeloid (macrophage, granulocyte, GM) colonies per 10<sup>4</sup> cells seeded, while erythroid colony forming potential was unaffected. (Fig. 5D). These results suggest that AHR<sup>-/-</sup> iPS-HSPCs harbor enhanced CFU potential compared with WT cells likely due to the increased proportion of progenitor-type (CD34<sup>+</sup>) cells present in the AHR<sup>-/-</sup> cultures.

In addition to the genetic approach noted above, a potent small molecule AHR inhibitor (CH-223191; CH) and a nontoxic AHR activator (FICZ), were used to modify AHR activity during differentiation in a stage-specific manner (Fig. 5A). To verify the efficacy of these small molecules, qPCR for the AHR target genes *CYP1A1* and *CYP1B1* was performed on D6 cells after 2 days of culture in control/+CH/+FICZ conditions. As expected, CH led to the efficient downregulation of *CYP1A1* and *CYP1B1* levels (approx. a 110- and 20-fold drop compared with control cells, respectively), while FICZ-treated cultures demonstrated a marked increase in target gene expression (approximately eight- and threefold, respectively) (Supporting Information Fig. S7A). These small molecules were then used to dissect the timepoints at which AHR activity impacts HSPC generation. Cells were exposed to CH or FICZ at specific developmental stages (D4–5: hem-endothelial mesoderm, D6+: hemogenic endothelium onwards, D4+ onwards), and the hematopoietic output was assessed by flow cytometry at D15. Neither CH or FICZ exposure between D4 and D5 significantly impacted iPS-HSPC cultures. In contrast, there were striking changes to the hematopoietic output of the cultures which were treated with small molecules from D6 onwards. In these assays, CH-treated cultures displayed increased proportions of CD34<sup>+</sup>CD45<sup>+</sup> cells (similar to the observations with AHR<sup>-/-</sup> cells), while treatment with FICZ had the opposite effect, with a marked decrease in the production of CD34<sup>+</sup>CD45<sup>+</sup> cells (Fig. 5E). These results indicate that stage-specific AHR repression from D6 onwards results in the increased generation and/or maintenance of hematopoietic progenitor cells in our iPS-HSPC differentiation system.

The mechanisms through which AHR inhibition/ablation causes an increase in primary HSPC expansion, for example, as observed in SR-1 treated human CB progenitor cells and other experimental systems, are currently not well defined. In the context of our iPS-HSPC system, we first asked whether the increase in hematopoietic progenitor cells was due to an increase in hematopoietic endothelial precursor cells which are present in D8 cultures as CD34<sup>+</sup>CD73<sup>+</sup>CXCR4<sup>-</sup> cells. Analyses of D8 WT and AHR<sup>-/-</sup> adherent cultures by flow cytometry showed no discernable change in the proportions of putative hemogenic endothelial cells, which comprise approximately 4%–6% of the cell population at this timepoint (Supporting Information Fig. S8A, S8B). Additionally, gene expression analyses of D8 cultures for a panel of hematopoietic progenitor markers at this timepoint indicated that gene expression was unchanged in AHR ablated cultures, with the exception of *CYP1B1* (Supporting Information Fig. S8C). Next, we assessed

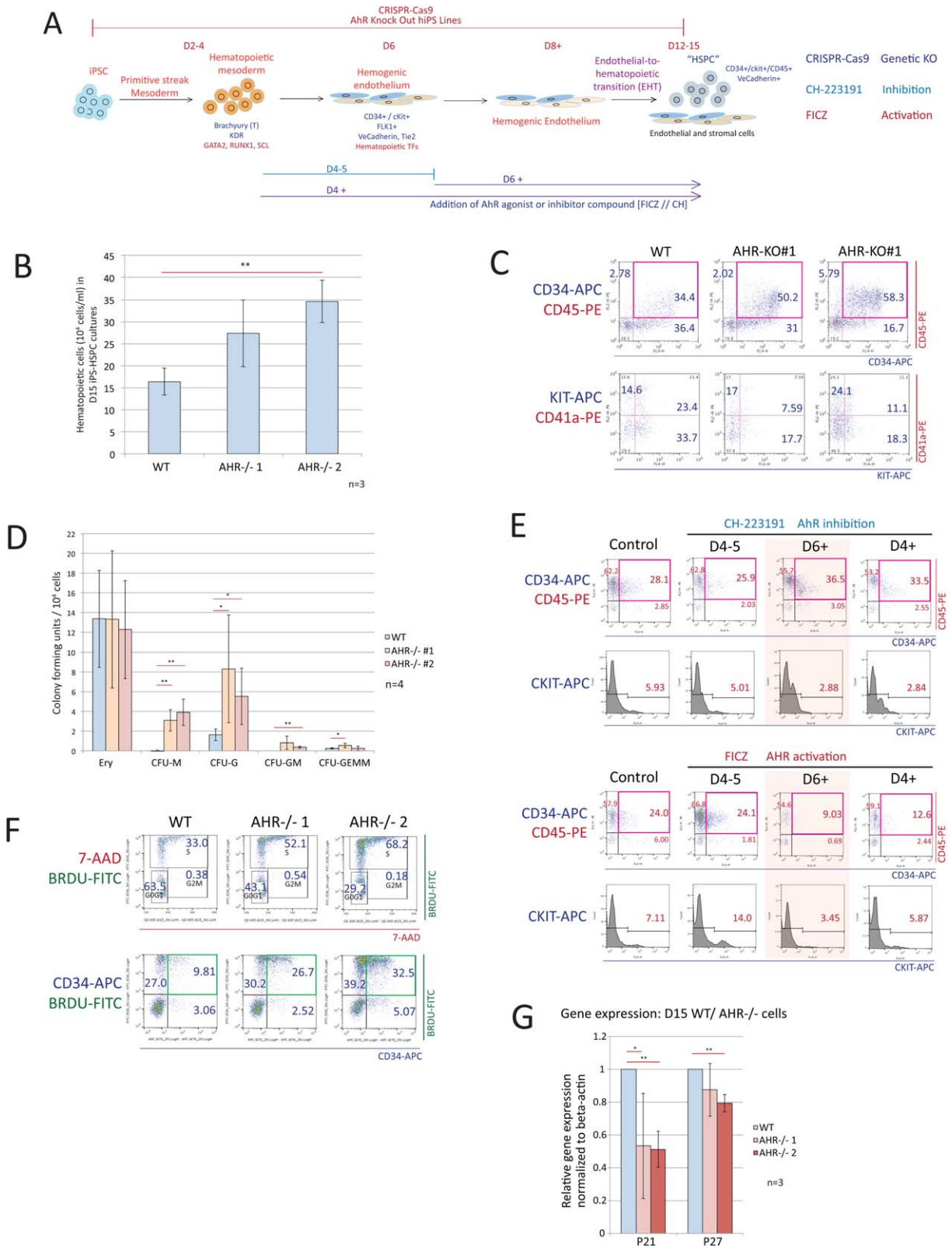


Figure 5.

whether the increase in iPS-HSPCs could be due to an increased rate of proliferation by testing WT and AHR<sup>-/-</sup> suspension hematopoietic cells in BrdU incorporation assays.

CD34 antibody-stained D16 HSPCs were assessed for BrdU positivity after 18 hours of culture with BrdU substrate. We observed that substantially more AHR<sup>-/-</sup> hematopoietic cells

were BrdU<sup>+</sup>, and that a greater proportion of the BrdU<sup>+</sup> cells were also CD34<sup>+</sup> compared with WT controls (Fig. 5F). These results suggest that CD34<sup>+</sup> AHR<sup>-/-</sup> iPS-HSPCs display increased proliferation rates compared with their WT counterparts, and that it is this increase in proliferation within the hematopoietic cell compartment, and not the hem-endothelial precursor cells, that largely accounts for the increased number of suspension hematopoietic cells in AHR<sup>-/-</sup> cultures. Gene expression analyses of WT and AHR<sup>-/-</sup> iPS-HSPCs reveal an approximate twofold decrease in levels of cell-cycle inhibitor cyclin dependent kinase inhibitor 1A (CDKN1A/P21) in the AHR<sup>-/-</sup> cells, which may account for the increased proliferative rate. Although it is currently unclear as to whether P21 is a direct target of AHR signaling in early hematopoietic cells, studies suggest a direct correlation between AHR signaling and P21 expression and functionality [58–60]. Finally, transcript levels of another cell cycle inhibitor CDKN1B/P27 were similarly reduced in WT and AHR<sup>-/-</sup> cells (Fig. 5G) – Notably, P27 has been shown to be a direct target of AHR in other systems [60, 61].

## DISCUSSION

While in vitro PSC-derived hematopoietic cells do not fully recapitulate aspects of developmental to adult-type hematopoiesis, transplantation studies with early mESC-derived mesoderm [62] and undifferentiated hPSCs and stromal cells [63, 64] indicate that both murine and human PSCs are functionally capable of giving rise to engraftable, long-term HSPCs via currently undefined mechanisms. In this study, we describe and characterize a step-wise, serum-free cytokine-driven monolayer iPSC-differentiation protocol that leads to the robust formation of hematopoietic progenitor cells with enhanced CFU potential and adult globin expression within the erythroid compartment in in vitro assays. This system is highly amenable to developmental, stage-specific modulation of signaling and can be used as a template in which to identify the molecular cues necessary for adult-type blood cell production. Using small molecule inhibitors, we demonstrate that Notch signaling, known to be crucial for the emergence of the first definitive hematopoietic cells in vivo but dispensable for primitive hematopoiesis, is necessary within the hematopoietic mesodermal stage to drive the downstream formation of iPS-derived hematopoietic progenitor

cells. Notch signaling is also required for the production of in vitro Erys with enhanced levels of  $\beta$ -globin expression. We also use this system to demonstrate that the AHR pathway plays a stage-specific role in hematopoietic progenitor cell derivation, and its modulation can be used to achieve increased numbers of hematopoietic progenitor cells.

Throughout these studies, we harnessed our ability to produce both primitive and putative definitive wave cells from the same parental iPSC lines to illustrate differences in signaling, expression patterning, and functionality in produced populations. As an example, increased levels of adult globin expression in the iPS-HSPC derived Erys when compared with iPS-MEP derived cells indicated that the iPS-HSPC differentiation system patterns development toward the formation of definitive-type hematopoietic progenitor cells. iPS-MEP-derived Erys are unable to upregulate  $\beta$ -globin in growth media where iHSPC-Ery cells can mature into abundant BFU-e and CFU-e colonies. Importantly, it is unknown whether increased  $\beta$ -globin transcripts within the iHSPC-Ery population represent a pan- or heterocellular distribution and this can be ascertained using single cell-based analyses.

We also used our defined systems to examine signaling pathways that impact definitive hematopoiesis. Notch signaling is critically important for lineage commitment and stem cell renewal, and it acts at multiple developmental and lineage-specific stages of blood development. *NOTCH1* and *NOTCH2* are implicated in developmental and adult hematopoiesis and act through multiple ligands including delta like (DLL) 1,3,4, Jagged (JAG) 1,2 to trigger the expression of Notch target genes such as *HES* and *HEY* that regulate cell fate, proliferation, and maturation. In vitro, *HES1* signaling via *NOTCH1* has been identified as a key signaling event that drives early hematopoietic commitment over endothelial cell fate from differentiating hPSCs [65]. There is increasing evidence that the careful manipulation of Notch signaling could be key to the in vitro derivation of definitive hematopoietic cells. Early, transient activation of the Notch signaling pathway via exogenous DL1 exposure is able to confer *HoxB4*-overexpressing mESC-derived HSPCs with definitive, multilineage engraftment potential, including T-cell and definitive erythroid potential [66]. Our stage-specific Notch inhibition experiments revealed a requirement for early-stage Notch signaling in the emergence of the iPS-HSPC population with D4–5 being the critical time window in our system at which Notch signaling is required for efficient EHT. In the Ery

**Figure 5.** Ablation of aryl hydrocarbon receptor (AHR) activity results in increased production of hematopoietic stem-progenitor cells (HSPCs) from induced pluripotent stem cells. **(A):** Schematic diagram outlining the genetic and stage-specific small molecule approaches to modulation of AHR activity during induced pluripotent stem (iPS)-HSPC development. **(B):** D15 iPS-HSPC suspension cell counts. Genetic ablation of AHR activity results in an increase in hematopoietic cell formation. Error bars = SD. Statistical significance determined by Student's *t* test analysis; \*,  $p \leq .05$ ; \*\*,  $p \leq .01$ . **(C):** Representative fluorescence-activated cell sorting (FACS) analyses of D15 wild-type (WT)/AHR<sup>-/-</sup> iPS-HSPC cultures. Increased proportions of AHR<sup>-/-</sup> hematopoietic cells are CD34<sup>+</sup>CD45<sup>+</sup> compared with WT cultures. cKIT<sup>+</sup> cells are also decreased in AHR<sup>-/-</sup> cultures. Representative plots from four independent experiments. **(D):** AHR<sup>-/-</sup> iPS-HSPCs display increased myeloid potential (macrophage and granulocyte lineages) in multi-lineage colony forming unit assays. Statistical significance determined by Student's *t* test analysis; \*,  $p \leq .05$ ; \*\*,  $p \leq .01$ . **(E):** Representative FACS analyses of D15 control/CH/6-formylindolo[3,2-b]carbazole (FICZ)-treated iPS-HSPC cultures. Inhibition of AHR (CH) from D6+ leads to the maintenance of the D15 CD34<sup>+</sup>CD45<sup>+</sup> iPS-HSPC population, while the opposite is true when the AHR is activated (FICZ). Modulation of AHR activity between D4–5 has no impact on iPS-HSPC formation. Representative plots from three independent experiments. **(F):** 5'-Bromo-2'-deoxyuridine incorporation assays reveal that AHR<sup>-/-</sup> iPS-HSPCs display an increased proliferative rate compared with WT iPS-derived cells. **(G):** Quantitative gene expression analyses reveal that the cell cycle regulator P21 (CDKN1A) is significantly downregulated in D15 AHR<sup>-/-</sup> hematopoietic cells. Results normalized to beta-actin. Statistical significance determined by Student's *t* test analysis; \*,  $p \leq .05$ ; \*\*,  $p \leq .01$ . Abbreviations: 7-AAD, 7-Aminoactinomycin D; AHR, aryl hydrocarbon receptor; BrdU, 5'-bromo-2'-deoxyuridine; CFU, colony forming unit; CH, CH223191; EHT, endothelial-to-hematopoietic transition; Ery, erythroid cell; FICZ, 6-formylindolo[3,2-b]carbazole; GATA2; HSPC, hematopoietic stem-progenitor cell; iPSC, induced pluripotent stem cell; KO, knockout; G, granulocyte; GM, granulocyte-macrophage; GEMM, granulocyte erythroid macrophage megakaryocyte; M, macrophage; RUNX1; SCL; WT, wild-type.

compartment, Notch signaling is required at both early (D4–5) and late stages (D6+) for the formation of Erys that are competent for  $\beta$ -globin gene expression. Expression levels of embryonic and fetal globin are unaffected by the absence of Notch. These results suggest that Notch may play a dual role in the definitive erythroid lineage, with an early requirement for formation of definitive hematopoietic progenitor cells, and possibly also a later role in the maintenance, expansion, or maturation of these cells into definitive Erys. It has previously been shown that Notch acts with erythropoietin to regulate levels of  $\beta$ -globin gene expression in an *in vitro* murine system [67]. Additionally, conditional loss-of-function *in vivo* murine experiments demonstrate that loss of both Notch1 and 2 has a negative impact on lineage commitment of adult HSPCs toward the erythroid lineage, while megakaryocyte potential is increased [68], suggesting a possible role for Notch in erythroid versus megakaryocyte fate decisions in the adult MEP precursor. DGE analyses of our D13 CD34<sup>+</sup> iPS-HSPCs revealed that Notch signaling was not overall differentially regulated compared with the primary FL or BM counterparts, suggesting that Notch is not underrepresented in the iPS-derived cells at this timepoint. Nevertheless, a transient increase in Notch signaling activation during the critical D4–5 time frame of hemogenic mesodermal development may further increase the definitive potential of the iPS-HSPCs derived from our system.

Although the AHR signaling cascade is less characterized than the Notch pathway in terms of its role in hematopoiesis, recent studies highlight how manipulation of this receptor may enhance the derivation of HSPCs from PSC sources. Unlike the Notch pathway which is critically important at multiple stages of developmental hematopoiesis, full genetic ablation of AHR signaling leads to relatively mild effects on adult hematopoiesis in murine models, indicating that it is not a crucial signaling pathway for the genesis or differentiation of hematopoietic cells. Indeed, loss of AHR appears to promote CD34<sup>+</sup> LSK HSPC generation in a circadian rhythm-dependent manner in young mice, although aged mice demonstrate stem cell exhaustion [34, 35]. Inhibition of this pathway in primary HSPCs has been shown to lead to the expansion and maintenance of stem-like progenitor cells [36], and more recently, there is evidence from the hPSC system that manipulation of this pathway can also result in increased numbers of stem-like hematopoietic cells. Our results indicate that genetic ablation of AHR activity leads to the increased expansion and maintenance of the iPS-derived HSPC population and the generation of approximately four times as many CD34<sup>+</sup>CD45<sup>+</sup> progenitor cells in AHR<sup>-/-</sup> cultures compared with WT. Complementary results using small molecule AHR modulators reveal that inhibition of AHR from D6 onwards is responsible for the increased proportions of CD34<sup>+</sup>CD45<sup>+</sup> cells [39, 40]. However, cell numbers and proliferative rates appear to be unaffected in contrast to results seen with AHR<sup>-/-</sup> iPS-HSPC cultures (Supporting Information Fig. S7). It is possible that the degree of AHR inhibition is not sufficient to fully replicate a complete genetic KO. Alternatively, AHR inhibition may be required at an earlier stage than D4 in our system to result in the downstream HSPC proliferative effect. Unlike other studies with AHR inhibitory compounds in the PSC system, we did not find evidence that AHR inhibition or ablation results in the expansion of hem-endothelial progenitor cell population [39, 40]. Instead,

our experiments show that the expansion observed in the AHR<sup>-/-</sup> iPS-HSPC population is due to an increased proliferative rate within this population, possibly due to the decreased transcriptional level of G1–S phase cell cycle regulators CDKN1A/P21 and CDKN1B/P27. We did not observe changes in the transcriptional globin profile of control and AHR<sup>-/-</sup> or small molecule-treated cells, indicating that perturbation of the AHR pathway during hematopoietic development had no bearing on the generation or the properties of the resultant erythroid lineage cells.

There is evidence in the literature that crosstalk between Notch and AHR occurs in other cell systems, with a positive regulatory relationship between these two pathways. The promoters of Notch1 and Notch2 carry AHR-binding elements and both genes are upregulated in the livers of AHR agonist (TCDD)-exposed mice [69]. Notch effector HES1 is positively regulated by AHR in a mammary carcinoma cell line [70] and in differentiating immortalized megakaryocytes [71], while Notch pathway genes Notch1, Notch3 and Hes1 have been shown to be vastly downregulated in the male reproductive organs of Ahr<sup>-/-</sup> mice [72]. We examined the expression of AHR and Notch pathway genes in our signaling-perturbed cells at D8–D15 and we did not observe gene expression changes that suggested signaling crosstalk upon targeting of either pathway (data not shown). This suggests a lack of crosstalk between AHR and Notch at these stages of the iPS-HSPC system. Nevertheless, our studies suggest that combinatorial modulation of both signaling pathways during hematopoietic differentiation leads to the efficient induction of definitive-lineage HSPCs from hPSCs.

## CONCLUSION

In this study, we used an induced pluripotent stem cell (iPSC)-based platform to demonstrate the critical, stage-specific roles of two key signaling pathways, Notch and the Aryl Hydrocarbon receptor, in the production of definitive blood cells. These results have broad implications for hematopoietic stem cell transplantation (HSCT) and clinical translation of iPSC-derived blood cells.

## ACKNOWLEDGMENTS

This work was supported by the NextGen Consortium U01HL107443 and R01HL133350 from the NIH/NHLBI, R01ES025409 from NIH/NIEHS and the Training Grant for Hematology 5T32 HL007501.

## AUTHOR CONTRIBUTIONS

A.L. and G.J.M.: conception and design, collection and/or assembly of data, data analysis and interpretation, manuscript writing; E.Z., N.S., K.V., T.A.M., Z.H.N., and Z.W.: collection and/or assembly of data; D.H.K.C.: data analysis and interpretation; M.H.S.: data analysis and interpretation, manuscript writing; D.H.S.: conception and design.

## DISCLOSURE OF POTENTIAL CONFLICTS OF INTEREST

M.H.S. declared research funding from Incyte. All other authors indicated no potential conflicts of interest.

## REFERENCES

- 1 Arora N, Wenzel PL, McKinney-Freeman SL et al. Effect of developmental stage of HSC and recipient on transplant outcomes. *Dev Cell* 2014; 29:621–628. doi:10.1016/j.devcel.2014.04.013.
- 2 Wang J, Wissink EM, Watson NB et al. Fetal and adult progenitors give rise to unique populations of CD8+ T cells. *Blood* 2016;128:3073–3082. doi:10.1182/blood-2016-06-725366.
- 3 Verovskaya E, Broekhuis MJC, Zwart E et al. Heterogeneity of young and aged murine hematopoietic stem cells revealed by quantitative clonal analysis using cellular barcoding. *Blood* 2013;122:523–532. doi:10.1182/blood-2013-01-481135.
- 4 Dykstra B, Kent D, Bowie M et al. Long-term propagation of distinct hematopoietic differentiation programs in vivo. *Cell Stem Cell* 2007; 1:218–229. doi:10.1016/j.stem.2007.05.015.
- 5 Ema H, Morita Y, Suda T. Heterogeneity and hierarchy of hematopoietic stem cells. *Exp Hematol* 2014;42:74–82.e2. doi:10.1016/j.exphem.2013.11.004.
- 6 Crisan M, Solaimani Kartalaei P, Neagu A et al. BMP and Hedgehog regulate distinct AGM hematopoietic stem cells ex vivo. *Stem Cell Rep* 2016;6:383–395. doi:10.1016/j.stemcr.2016.01.016.
- 7 Kennedy M, Awong G, Sturgeon CM et al. T lymphocyte potential marks the emergence of definitive hematopoietic progenitors in human pluripotent stem cell differentiation cultures. *Cell Rep* 2012;2:1722–1735. doi:10.1016/j.celrep.2012.11.003.
- 8 Sturgeon CM, Ditadi A, Awong G et al. Wnt signaling controls the specification of human pluripotent stem cells. *Nat Biotechnol* 2014;32:554–561. doi:10.1038/nbt.2915.
- 9 Uenishi G, Theisen D, Lee J-H et al. Tenascin C promotes hematoendothelial development and T lymphoid commitment from human pluripotent stem cells in chemically defined conditions. *Stem Cell Rep* 2014;3:1073–1084. doi:10.1016/j.stemcr.2014.09.014.
- 10 Chang C-J, Mitra K, Koya M et al. Production of embryonic and fetal-like red blood cells from human induced pluripotent stem cells. *PLoS ONE* 2011;6:e25761. doi:10.1371/journal.pone.0025761.
- 11 Olivier E, Qiu C, Bouhassira EE. Novel, high-yield red blood cell production methods from CD34-positive cells derived from human embryonic stem, yolk sac, fetal liver, cord blood, and peripheral blood. *STEM CELLS TRANS-LATIONAL MEDICINE* 2012;1:604–614. doi:10.5966/sctm.2012-0059.
- 12 Vodyanik MA, Bork JA, Thomson JA et al. Human embryonic stem cell-derived CD34+ cells: Efficient production in the coculture with OP9 stromal cells and analysis of lymphohematopoietic potential. *Blood* 2005;105:617–626. doi:10.1182/blood-2004-04-1649.
- 13 Dias J, Gumenyuk M, Kang H et al. Generation of red blood cells from human induced pluripotent stem cells. *Stem Cells Dev* 2011;20:1639–1647. doi:10.1089/scd.2011.0078.
- 14 Hattangadi SM, Wong P, Zhang L et al. From stem cell to red cell: Regulation of erythropoiesis at multiple levels by multiple proteins, RNAs, and chromatin modifications. *Blood* 2011;118:6258–6268. doi:10.1182/blood-2011-07-356006.
- 15 Lis R, Karrasch CC, Poulos MG et al. Conversion of adult endothelium to immunocompetent haematopoietic stem cells. *Nature* 2017;545:439–445. doi:10.1038/nature22326.
- 16 Sugimura R, Jha DK, Han A et al. Haematopoietic stem and progenitor cells from human pluripotent stem cells. *Nature* 2017; 545:432–438. doi:10.1038/nature22370.
- 17 Doulatov S, Vo LT, Chou SS et al. Induction of multipotential hematopoietic progenitors from human pluripotent stem cells via respecification of lineage-restricted precursors. *Cell Stem Cell* 2013;13:459–470. doi:10.1016/j.stem.2013.09.002.
- 18 Pearson S, Sroczyńska P, Lacaud G et al. The stepwise specification of embryonic stem cells to hematopoietic fate is driven by sequential exposure to Bmp4, activin A, bFGF and VEGF. *Dev Camb Engl* 2008;135:1525–1535. doi:10.1242/dev.011767.
- 19 Lengerke C, Schmitt S, Bowman TV et al. BMP and Wnt specify hematopoietic fate by activation of the Cdx-Hox pathway. *Cell Stem Cell* 2008;2:72–82. doi:10.1016/j.stem.2007.10.022.
- 20 Nostro MC, Cheng X, Keller GM et al. Wnt, activin, and BMP signaling regulate distinct stages in the developmental pathway from embryonic stem cells to blood. *Cell Stem Cell* 2008;2:60–71. doi:10.1016/j.stem.2007.10.011.
- 21 Ng ES, Azzola L, Bruveris FF et al. Differentiation of human embryonic stem cells to HOXA(+) hemogenic vasculature that resembles the aorta-gonad-mesonephros. *Nat Biotechnol* 2016;34:1168–1179. doi:10.1038/nbt.3702.
- 22 de Bruijn MFTR, Ma X, Robin C et al. Hematopoietic stem cells localize to the endothelial cell layer in the midgestation mouse aorta. *Immunity* 2002;16:673–683.
- 23 Medvinsky A, Dzierzak E. Definitive hematopoiesis is autonomously initiated by the AGM region. *Cell* 1996;86:897–906.
- 24 Sánchez MJ, Holmes A, Miles C et al. Characterization of the first definitive hematopoietic stem cells in the AGM and liver of the mouse embryo. *Immunity* 1996;5:513–525.
- 25 Bertrand JY, Cisson JL, Stachura DL et al. Notch signaling distinguishes 2 waves of definitive hematopoiesis in the zebrafish embryo. *Blood* 2010;115:2777–2783. doi:10.1182/blood-2009-09-244590.
- 26 Hadland BK, Huppert SS, Kanungo J et al. A requirement for Notch1 distinguishes 2 phases of definitive hematopoiesis during development. *Blood* 2004;104:3097–3105. doi:10.1182/blood-2004-03-1224.
- 27 Robert-Moreno A, Espinosa L, de la Pompa JL et al. RBPjkappa-dependent Notch function regulates Gata2 and is essential for the formation of intra-embryonic hematopoietic cells. *Dev Camb Engl* 2005;132:1117–1126. doi:10.1242/dev.01660.
- 28 Kumano K, Chiba S, Kunisato A et al. Notch1 but not Notch2 is essential for generating hematopoietic stem cells from endothelial cells. *Immunity* 2003;18:699–711.
- 29 Gering M, Patient R. Notch signalling and haematopoietic stem cell formation during embryogenesis. *J Cell Physiol* 2010; 222:11–16. doi:10.1002/jcp.21905.
- 30 McKinney-Freeman S, Cahan P, Li H et al. The transcriptional landscape of hematopoietic stem cell ontogeny. *Cell Stem Cell* 2012;11:701–714. doi:10.1016/j.stem.2012.07.018.
- 31 Gori JL, Butler JM, Chan Y-Y et al. Vascular niche promotes hematopoietic multipotent progenitor formation from pluripotent stem cells. *J Clin Invest* 2015;125:1243–1254. doi:10.1172/JCI79328.
- 32 Smith BW, Rozelle SS, Leung A et al. The aryl hydrocarbon receptor directs hematopoietic progenitor cell expansion and differentiation. *Blood* 2013;122:376–385. doi:10.1182/blood-2012-11-466722.
- 33 Singh KP, Casado FL, Opanashuk LA et al. The aryl hydrocarbon receptor has a normal function in the regulation of hematopoietic and other stem/progenitor cell populations. *Biochem Pharmacol* 2009;77:577–587. doi:10.1016/j.bcp.2008.10.001.
- 34 Singh KP, Garrett RW, Casado FL et al. Aryl hydrocarbon receptor (AhR)-null allele mice have abnormal characteristics and functions of hematopoietic stem/progenitor cells. *Stem Cells Dev* 2011;20:769. September doi:10.1089/scd.2010.0333.
- 35 Singh KP, Bennett JA, Casado FL et al. Loss of aryl hydrocarbon receptor promotes gene changes associated with premature hematopoietic stem cell exhaustion and development of a myeloproliferative disorder in aging mice. *Stem Cells Dev* October 2013; doi:10.1089/scd.2013.0346.
- 36 Boitano AE, Wang J, Romeo R et al. Aryl hydrocarbon receptor antagonists promote the expansion of human hematopoietic stem cells. *Science* 2010;329:1345–1348. doi:10.1126/science.1191536.
- 37 Fares I, Chagraoui J, Gareau Y et al. Cord blood expansion. Pyrimidoindole derivatives are agonists of human hematopoietic stem cell self-renewal. *Science* 2014;345:1509–1512. doi:10.1126/science.1256337.
- 38 Fares I, Chagraoui J, Lehnertz B et al. EPCR expression marks UM171-expanded CD34(+) cord blood stem cells. *Blood* 2017; 129:3344–3351. doi:10.1182/blood-2016-11-750729.
- 39 Angelos MG, Ruh PN, Webber BR et al. Aryl hydrocarbon receptor inhibition promotes hematolymphoid development from human pluripotent stem cells. *Blood* 2017;129:3428–3439. doi:10.1182/blood-2016-07-730440.
- 40 Li X, Xia C, Wang T et al. Pyrimidoindole derivative UM171 enhances derivation of hematopoietic progenitor cells from human pluripotent stem cells. *Stem Cell Res* 2017; 21:32–39. doi:10.1016/j.scr.2017.03.014.
- 41 Gianotti-Sommer A, Rozelle SS, Sullivan S, et al. Generation of human induced pluripotent stem cells from peripheral blood using the STEMCCA lentiviral vector. In: *StemBook*. Cambridge, MA: Harvard Stem Cell Institute, 2013. <http://www.ncbi.nlm.nih.gov/books/NBK133275/>.
- 42 Somers A, Jean J-C, Sommer CA et al. Generation of transgene-free lung disease-specific human induced pluripotent stem cells using a single excisable lentiviral stem cell cassette. *Stem Cells Dayt Ohio* 2010;28:1728–1740. doi:10.1002/stem.495.
- 43 Ivanovs A, Rybtsov S, Anderson RA et al. Identification of the Niche and Phenotype of

the First Human Hematopoietic Stem Cells. *Stem Cell Rep* 2014;2:449–456. doi:10.1016/j.stemcr.2014.02.004.

- 44** Ditadi A, Sturgeon CM, Tober J et al. Human definitive haemogenic endothelium and arterial vascular endothelium represent distinct lineages. *Nat Cell Biol* 2015;17:580–591. doi:10.1038/ncb3161.
- 45** Ditadi A, Sturgeon CM. Directed differentiation of definitive hemogenic endothelium and hematopoietic progenitors from human pluripotent stem cells. *Methods San Diego Calif* 2016;101:65–72. doi:10.1016/j.jmeth.2015.10.001.
- 46** Yang L, Bryder D, Adolfsson J et al. Identification of Lin(-)Sca1(+)/Kit(+)/CD34(+)/Flt3-short-term hematopoietic stem cells capable of rapidly reconstituting and rescuing myeloablanted transplant recipients. *Blood* 2005;105:2717–2723. doi:10.1182/blood-2004-06-2159.
- 47** Adolfsson J, Månsson R, Buza-Vidas N et al. Identification of Flt3+ lympho-myeloid stem cells lacking erythro-megakaryocytic potential: a revised road map for adult blood lineage commitment. *Cell* 2005;121:295–306. doi:10.1016/j.cell.2005.02.013.
- 48** Sankaran VG, Xu J, Ragoczy T et al. Developmental and species-divergent globin switching are driven by BCL11A. *Nature* 2009;460:1093–1097. doi:10.1038/nature08243.
- 49** Vinjamur DS, Alhashem YN, Mohamad SF et al. Krüppel-like transcription factor KLF1 is required for optimal  $\gamma$ - and  $\beta$ -globin expression in human fetal erythroblasts. *PLoS One* 2016;11:e0146802. doi:10.1371/journal.pone.0146802.
- 50** Zhou D, Liu K, Sun C-W et al. KLF1 regulates BCL11A expression and gamma- to beta-globin gene switching. *Nat Genet* 2010;42:742–744. doi:10.1038/ng.637.
- 51** Kurita R, Suda N, Sudo K et al. Establishment of immortalized human erythroid progenitor cell lines able to produce enucleated red blood cells. *PLoS One* 2013;8:e59890. doi:10.1371/journal.pone.0059890.
- 52** Burns CE, Traver D, Mayhall E et al. Hematopoietic stem cell fate is established by the Notch-Runx pathway. *Genes Dev* 2005;19:2331–2342. doi:10.1101/gad.1337005.
- 53** Krebs LT, Xue Y, Norton CR et al. Notch signaling is essential for vascular morphogenesis in mice. *Genes Dev* 2000;14:1343–1352. doi:10.1101/gad.14.11.1343.
- 54** Laranjeiro R, Alcobia I, Neves H et al. The notch ligand delta-like 4 regulates multiple stages of early hemato-vascular development. *PLoS One* 2012;7:e34553. doi:10.1371/journal.pone.0034553.
- 55** Lawson ND, Scheer N, Pham VN et al. Notch signaling is required for arterial-venous differentiation during embryonic vascular development. *Dev Camb Engl* 2001;128:36753683.
- 56** Chen MJ, Yokomizo T, Zeigler BM et al. Runx1 is required for the endothelial to haematopoietic cell transition but not thereafter. *Nature* 2009;457:887–891. doi:10.1038/nature07619.
- 57** Nakagawa M, Ichikawa M, Kumano K et al. AML1/Runx1 rescues Notch1-null mutation-induced deficiency of para-aortic splanchnopleural hematopoiesis. *Blood* 2006;108:3329–3334. doi:10.1182/blood-2006-04-019570.
- 58** Koliopoulos A, Kleeff J, Xiao Y et al. Increased arylhydrocarbon receptor expression offers a potential therapeutic target for pancreatic cancer. *Oncogene* 2002;21:6059–6070. doi:10.1038/sj.onc.1205633.
- 59** O'Donnell EF, Jang HS, Pearce M et al. The aryl hydrocarbon receptor is required for induction of p21cip1/waf1 expression and growth inhibition by SU5416 in hepatoma cells. *Oncotarget* 2017;8:25211–25225. doi:10.18632/oncotarget.16056.
- 60** Pang P-H, Lin Y-H, Lee Y-H et al. Molecular mechanisms of p21 and p27 induction by 3-methylcholanthrene, an aryl-hydrocarbon receptor agonist, involved in antiproliferation of human umbilical vascular endothelial cells. *J Cell Physiol* 2008;215:161–171. doi:10.1002/jcp.21299.
- 61** Kolluri SK, Weiss C, Koff A et al. p27(Kip1) induction and inhibition of proliferation by the intracellular Ah receptor in developing thymus and hepatoma cells. *Genes Dev* 1999;13:1742–1753.
- 62** Pearson S, Cuvertino S, Fleury M et al. In vivo repopulating activity emerges at the onset of hematopoietic specification during embryonic stem cell differentiation. *Stem Cell Rep* 2015;4:431–444. doi:10.1016/j.stemcr.2015.01.003.
- 63** Amabile G, Welner RS, Nombela-Arrieta C et al. In vivo generation of transplantable human hematopoietic cells from induced pluripotent stem cells. *Blood* 2013;121:1255–1264. doi:10.1182/blood-2012-06-434407.
- 64** Suzuki N, Yamazaki S, Yamaguchi T et al. Generation of engraftable hematopoietic stem cells from induced pluripotent stem cells by way of teratoma formation. *Mol Ther J Am Soc Gene Ther* 2013;21:1424–1431. doi:10.1038/mt.2013.71.
- 65** Lee JB, Werbowetski-Ogilvie TE, Lee J-H et al. Notch-HES1 signaling axis controls hemato-endothelial fate decisions of human embryonic and induced pluripotent stem cells. *Blood* 2013;122:1162–1173. doi:10.1182/blood-2012-12-471649.
- 66** Lu Y-F, Cahan P, Ross S et al. Engineered murine HSCs reconstitute multi-lineage hematopoiesis and adaptive immunity. *Cell Rep* 2016;17:3178–3192. doi:10.1016/j.celrep.2016.11.077.
- 67** Henning K, Schroeder T, Schwanbeck R et al. mNotch1 signaling and erythropoietin cooperate in erythroid differentiation of multipotent progenitor cells and upregulate beta-globin. *Exp Hematol* 2007;35:1321–1332. doi:10.1016/j.jephem.2007.05.014.
- 68** Oh P, Lobry C, Gao J et al. In vivo mapping of notch pathway activity in normal and stress hematopoiesis. *Cell Stem Cell* 2013;13:190–204. doi:10.1016/j.stem.2013.05.015.
- 69** Lee JS, Cella M, McDonald KG et al. AHR drives the development of gut ILC22 cells and postnatal lymphoid tissues via pathways dependent on and independent of Notch. *Nat Immunol* 2011;13:144–151. doi:10.1038/ni.2187.
- 70** Thomsen JS, Kietz S, Ström A et al. HES-1, a novel target gene for the aryl hydrocarbon receptor. *Mol Pharmacol* 2004;65:165–171. doi:10.1124/mol.65.1.165.
- 71** Lindsey ST, Papoutsakis E. The aryl hydrocarbon receptor (AHR) transcription factor regulates megakaryocytic polyploidization. *Br J Haematol* 2011;152:469–484. doi:10.1111/j.1365-2141.2010.08548.x.
- 72** Huang B, Butler R, Miao Y et al. Dysregulation of Notch and ER $\alpha$  signaling in AhR male mice. *Proc Natl Acad Sci USA* 2016;113:11883–11888. doi:10.1073/pnas.1613269113.



See [www.StemCells.com](http://www.StemCells.com) for supporting information available online.